FABRIC-FORMED CONCRETE PANEL DESIGN

by

Robert P. Schmitz, P.E.

A Report Submitted to the Faculty of the

Milwaukee School of Engineering

in Partial Fulfillment of the

Requirements for the Degree of

Master of Science in Structural Engineering

Milwaukee, Wisconsin

25 October 2004

ABSTRACT

Concrete wall panels have traditionally been cast using a rigid formwork. Straight-forward methods of analysis and design are available for the traditionally cast concrete wall or floor panel. This is not so for the panel cast in a flexible fabric formwork. The purpose of this report is to develop a design procedure that allows one to design a fabric cast concrete panel.

A four-step procedure for analytically modeling the fabric formwork is developed in order to determine the final shape of the concrete wall panel. The structural analysis program ADINA was employed to analyze the complexities of a flexible fabric formwork and the concrete panel cast in it.

Analytical modeling and design techniques are developed in this report that will allow the design community another way to express themselves through the use of flexible fabric formwork.

ACKNOWLEDGMENTS

The author wishes to express his sincere appreciation to Professor Peter Huttelmaier, Ph.D. who served as my advisor and committee member for this project and to Professors Richard DeVries, Ph.D. and Mahmoud Maamouri, Ph.D. for their assistance in the preparation of this manuscript. In addition, special thanks go to Professor Mark West, Director of the Centre for Architectural Structures Technology (C.A.S.T.) of the University of Manitoba, whose work on fabric-cast concrete wall panels provided the inspiration for this project.

The author also wishes to thank my wife, Geri, whose efforts in proofing this manuscript were most appreciated. I will forever be in her debt.

TABLE OF CONTENTS

Section 4 – Step 4 – Panel Design and Discussion

Section 5 – Conclusions and Recommendations

LIST OF FIGURES

LIST OF FIGURES – APPENDIX A

LIST OF FIGURES – APPENDIX B

LIST OF FIGURES – APPENDIX C

LIST OF FIGURES – APPENDIX D

LIST OF TABLES

NOTATION/GLOSSARY

b	Creep coefficient for geotextile
E	Modulus of Elasticity of slurry material, psi
E_a	Modulus of Elasticity in local y axis for 2-D Solid fabric element, psi
E_b	Modulus of Elasticity in local z axis for 2-D Solid fabric element, psi
E_c	Modulus of Elasticity for concrete, psi
E_{tc}	Initial Tangent Modulus of Elasticity for concrete, psi
E_{fill}	Modulus of Elasticity in geotextile's cross machine direction, psi
E_{warp}	Modulus of Elasticity in geotextile's machine direction, psi
E_s	Modulus of Elasticity for reinforcing steel, psi
E_{ts}	Strain Hardening (Tangent) Modulus of Elasticity for reinforcing steel, psi
D_c	Density for concrete, lb-s^2/in^4
D_{sm}	Density for slurry material, lb-s^2/in^4
D_s	Density for reinforcing steel, lb-s^2/in^4
f'_c	28 day strength of concrete, psi
f'_{uc}	Ultimate strength of concrete, psi
f_r	Modulus of rupture for concrete, psi
f_y	Strength of reinforcing steel, psi
G	Shear Modulus, psi
t	thickness, inches or time, hrs
wt_c	Weight of concrete, lbs/ft^3
wt_{sm}	Weight of slurry material, lbs/ft^3
wt_s	Weight of reinforcing steel, lbs/ft^3
ε	Strain, %
ε_c	Compressive strain of concrete
ε_{uc}	Ultimate compressive strain of concrete
ε_t	Total strain, %
ε_0	Initial strain, %
Φ_p	Strength reduction factor for plain concrete
σ	Normal stress
ν	Poisson's Ratio for geotextile
ν_c	Poisson's Ratio for concrete
ν_{sm}	Poisson's Ratio for slurry material
ν_s	Poisson's Ratio for reinforcing steel

Slurry.	Plastic concrete material used in Finite Element Analysis (FEA) model.
Fill.	Cross machine direction of geotextile fabric.
Warp.	Machine direction of geotextile fabric.

SECTION 1 – INTRODUCTION

1.1 Background

The use of a flexible formwork for the purpose of casting concrete appears contrary to the way concrete has traditionally been cast, i.e. casting in an all-rigid formwork, but the casting of concrete in a flexible formwork is beginning to attract attention as a method of construction. An article by Mark West, Director of the Centre for Architectural Structures Technology (C.A.S.T.) at the University of Manitoba, Canada, published in *Concrete International* caught the author's attention with regard to how this method of construction might be utilized and engineered [1]. Upon further inquiry, correspondence with Professor West and a visit to C.A.S.T., on the University of Manitoba campus, the author was brought current on the state-of-the-art for this method of construction.

Professor West and his architectural students at C.A.S.T. have been exploring the use of flexible formwork for casting concrete wall panels [2]. The form a wall panel might take is first explored using a plaster model with various interior and perimeter boundary conditions. The cloth fabric, when draped over interior supports, deforms as gravity forms the shape of the panel. Once a satisfactory design has been obtained a full-scale cast with concrete can be made.

The casting of a full-scale panel using concrete requires finding a fabric capable of supporting the weight of the wet concrete. For this purpose a geotextile fabric made of woven polypropylene fibers was utilized. The flexible fabric material was pre-tensioned in the framework and assorted interior supports were added. Depending upon the

configuration of these interior support conditions, three-dimensional funicular tension curves were produced in the fabric as it deformed under the weight of the wet concrete. Reinforcement added to the panels only served to hold them together and was not for any particular design load condition.

For a building project, a wall panel may be required for purely functional reasons, such as resisting the required lateral loads and keeping the weather out. Adding to these requirements a wall panel may, for architectural reasons, be required to be expressive in the form it takes. The potential benefits for using a flexible fabric formwork include: increased freedom of design expression; a design where "form follows function"; economies of construction; and improvement in the finish and durability of the product. The challenge, from an engineering perspective, is finding a method to analyze the complex structural shape a wall panel may ultimately take.

1.2 Purpose of Report

Straight-forward methods of analysis and design are available for the traditionally cast concrete wall or floor panel. This is not so for the panel cast in a flexible fabric formwork. The final panel form, performance and function of the fabric membrane and the reinforcement of the panel for design loads all add to the complexities of panel analysis and design. To date, no design procedures or method to predict the deflected shape of a fabric cast panel have been developed.

The purpose of this report is to develop a procedure that allows one to design a fabric cast

concrete panel. A four-step procedure for analytically modeling the fabric formwork, loaded with the plastic concrete, is developed in order to determine the final shape of the concrete wall panel. These steps are:

1. Determine the paths the lateral loads take to the points where the wall panel is to be anchored.
2. Using the load paths, defined in Step 1, model the fabric and plastic concrete material as 2-D and 3-D Solid elements, respectively. These elements define the panel's lines of support.
3. "Form-find" the final shape of the panel by incrementally increasing the 3-D concrete elements until equilibrium in the supporting fabric formwork has been reached.
4. Analyze and design the panel for strength requirements to resist the lateral live load and self-weight dead load being imposed upon it.

As noted above, economies of construction are available with this method of construction. It is expected that by utilizing the above four-step procedure, obtaining an optimal panel shape is possible. The implication is that the above procedure becomes an iterative process. If, after a strength analysis of the panel is made in Step 4, it is found that the panel is either "under-strength" or too far "over-strength" adjustments to the model in Step 2 will be required and Steps 3 and 4 repeated. Prior to implementing this four-step procedure, however, the modeling techniques utilized in steps two and three above must first be defined.

SECTION 2 – LITERATURE REVIEW

2.1 Fabric Cast Panels

The focus of this project and report is the development of a design procedure which will allow one to design a fabric cast concrete panel. The primary source on the subject of fabric casting concrete are the works of Professor Mark West of the University of Manitoba who has been involved with this method of casting concrete for more than ten years. Articles written by Professor West give an introduction, a history and an outline of the benefits using the fabric formwork method of construction for casting not only concrete wall panels, but other structural shapes as well, such as beams and columns [1, 2, 3, 4, 5, 6, 7]. While not the focus of this report, it should be noted that the use of fabric for a formwork is not limited to these common structural shapes. Fabric formwork has also been used for foundations, revetments, underwater pile jackets and pond liners.

2.2 Geotextile Fabrics

The geosynthetic material used by Professor West and his students for casting concrete is a woven polypropylene plastic. This material is commonly used as soil reinforcement in geotechnical projects such as paving roadways, retaining walls, slope stabilization and pond liners for waste management projects.

Sources used for technical information on this product included Technical Notes and Bulletins by Amoco [8, 9] whose Propex 2006 product was used by the C.A.S.T. students, technical papers published in *Geosynthetics International* [10, 11] and standard methods of testing by ASTM International [12]. Additional sources of information were available

"online" from the Geosynthetic Research Institute, Drexel University, Folsom, PA. [13].

2.3 Developments in Finite Element Methods

Computer programs in structural analysis have advanced immensely in recent years. While a complete survey of finite element methods and programs is beyond the scope of this report some of the features available in the program used in this report, ADINA (Automatic, Dynamic, Incremental, Nonlinear, Analysis), are worth mentioning [14, 15, 16]. ADINA is capable of not only analyzing structures but also fluid, fluid flows with structural interaction, heat transfer and field problems, and thermo-mechanical coupling.

For the problem at hand the ability to model isotropic as well as orthotropic material and material nonlinearity with large deformations was important and required. In addition, the ability to adjust the geometry for the 3-D Solid elements was crucial in defining the final shape the concrete panel would take. The program also allowed one to define initial strains in the flexible fabric formwork and was an indispensable feature. Very detailed definitions of materials, such as concrete, make the program well suited to analyzing complex concrete panel shapes, as presented in this report.

The publication *Finite Element Procedures* (Prentice-Hall, 1996) by K.J. Bathe, author of ADINA, was helpful in explaining the theory behind some of the complex features used in this program [17].

SECTION 3 – MATERIALS AND ANALYSIS METHODOLOGY

3.1 Finite Element Analysis (FEA) Model Development

Model development and analysis of the fabric cast concrete panel was performed utilizing the structural analysis/finite element program ADINA [14, 15, 16]. The strategy that was employed in the development of the finite element model was one where efficient modeling played a key role. Ideally, one would like to define in the same model, the elements making up the supporting fabric formwork and the elements which eventually make up the final concrete panel shape. Once the final concrete panel shape was defined by using an iterative "form-finding" technique, the fabric elements were discarded and the concrete panel elements designed for the appropriate lateral loads. While a surface load representing the weight of the concrete could be used to define the shape of the panel using the same iterative procedure, it would not be as efficient as the proposed method.

The difficulty with combining these two element types in the same model is that they each have their own material properties which can contribute to the overall strength of the model. Initially, the concrete is plastic and is considered to be fluid in nature, similar to slurry. The slurry contributes weight to the fabric element portion of the model but cannot be allowed to contribute any stiffness to it. An intermediate step is required using this slurry like material that has weight, but no strength, as the material property for the concrete panel elements while the final panel shape is being found. Model development and verification of the "form-finding" technique are carried out for a 4'-0" x 8'-0" x 4" thick demonstration panel in Sections 3.3 and 3.4.

3.1.1 Model Panel Definitions

Model development and examples for this report required the use of a number of panel configurations. Panel design series are tracked by number: **Panel 1**, **Panel 2**, **Panel 3**, etc. The use of an iterative design procedure required designs be tracked within a series as well. Iterative panel designs within a series are numbered: **Panel 1a**, **Panel 1b**, **Panel 1c**, etc.

The **Panel 1** series was used to define and track analysis results from the Fabric Model in Section 3.2 and procedure verification using a Control Model in Section 3.4. The Combined Fabric and Slurry Model in Section 3.3 used **Panel 2** series to track analysis results. **Panel 3** series was used to describe each of the panel boundary conditions that were considered for the Load Path study described in Section 3.5.1. **Panel 4, 5 and 6** series were used to define the three panel configurations considered for design in Section 3.5.2 and track their analysis results in Section 4 using the four-step procedure developed in this report.

3.2 The Fabric Model

3.2.1 Advantages and Disadvantages of Geotextile Fabric as Formwork Material

Advantages include:

1. Very complex shapes are possible. Designs are limited only by one's imagination.
2. Geotextile fabric is strong, lightweight and inexpensive.
3. Economies of construction may be realized as less concrete and reinforcing are required with a more efficient design.
4. Improved durability and surface finish in the final concrete product are possible due to the filtering of air bubbles and excess bleed water through the fabric.

Disadvantages include:

1. There is the potential for creep. Relaxation can occur due to the prestress forces in the membrane. Creep can also be accelerated by an increase in temperature such as might occur due to hydration in the concrete as it cures.
2. The concrete has to be placed carefully and the fabric formwork must not be jostled while the concrete is in a plastic state.

3.2.2 Material Properties of Geotextile Fabrics

The material is orthotropic. The modulus of elasticity is different in the machine direction (along the length of the roll) and the cross-machine direction (width of the roll). These differences are important when modeling the fabric as well as for securing it to the supporting formwork. Mechanical properties for geotextile fabrics are obtained from stress-strain curves developed in accordance with the standard test methods of ASTM D4595 [12]. A stress-strain curve is required for each direction of the material, WARP (machine direction) and FILL (cross machine direction). Depending upon the appearance of the material's stress-strain curve a determination is made whether a Hookean (linear) region exists or not. Based on this determination the initial, tangent and offset (or secant) tensile modulus may be constructed. The appendixes of ASTM D4595 provide guidance on the construction of these tensile moduli.

Stress-strain data for the Amoco 2006 geotextile fabric was obtained from Amoco Fabrics and Fibers Company. Figure 1 shows the stress-strain curves resulting from tests conducted by Amoco. Using the appendixes of ASTM D4595 as a guide the author has constructed the initial, tangent and secant tensile moduli. Information obtained from Figure 1 allowed the following properties for this *elastic-orthotropic* material to be entered into the

computer model (See Table 1).

Table 1. Amoco 2006 Geotextile Fabric Material Properties.

t = 0.03 in	Fabric thickness
$E_{fill} = E_b = 93{,}333$ psi	Modulus of Elasticity, Cross Machine Direction
$E_{warp} = E_a = 47{,}667$ psi	Modulus of Elasticity, Machine Direction
G = 23,833 psi	Shear Modulus
$\nu = 0.0$	Poisson's Ratio

There is little interaction between the two perpendicular directions in a woven fabric and a value of zero for Poisson's Ratio was chosen for this model [10].

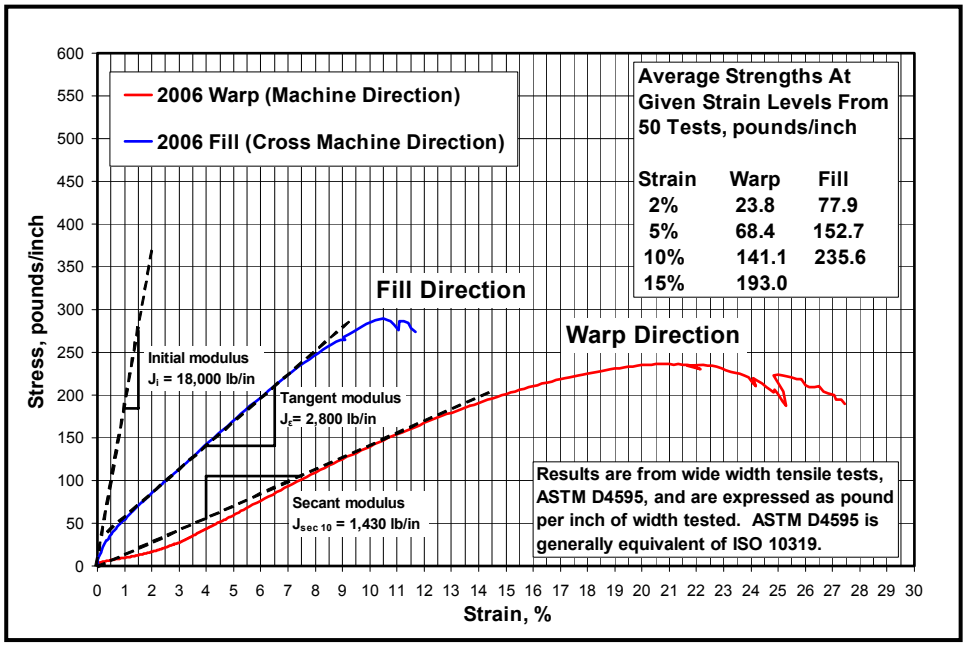

Figure 1. Amoco 2006 Stress-Strain Curves and Tensile Moduli [18].

3.2.3 Creep in Geotextile Fabrics

The effects of creep in the geotextile fabric will not be included in the modeling of the fabric panel for this report. For a general discussion and as a point of reference for future considerations see Appendix A.

3.2.4 ADINA Model Panel 1

Panel 1 in the ADINA computer model represents the supporting fabric formwork using 2-D Solid elements as shown in Figure 2. The 2-D Solid element uses a 3-D plane stress (membrane) kinematic assumption.

A prestress load of 2% is applied to the fabric in each direction. Boundary reactions due to this prestress load are shown in Figure 3. As a result of the 2% prestress load the strain in the fabric is 0.02 in each direction and the resulting stresses are found by

$$\sigma_a = E_a \varepsilon_a = 953.3 \text{ psi} \quad \text{(Machine Direction)}, \tag{1}$$

$$\sigma_b = E_b \varepsilon_b = 1866.7 \text{ psi} \quad \text{(Cross Machine Direction)} \tag{2}$$

where

E_a Modulus of Elasticity in the Machine Direction,
E_b Modulus of Elasticity in the Cross Machine Direction,
ε_a strain in the Machine Direction,
ε_b strain in the Cross Machine Direction.

Reactions per unit length, as shown in Figure 3, are found by taking stress times fabric thickness, thus

$$R = \sigma t. \tag{3}$$

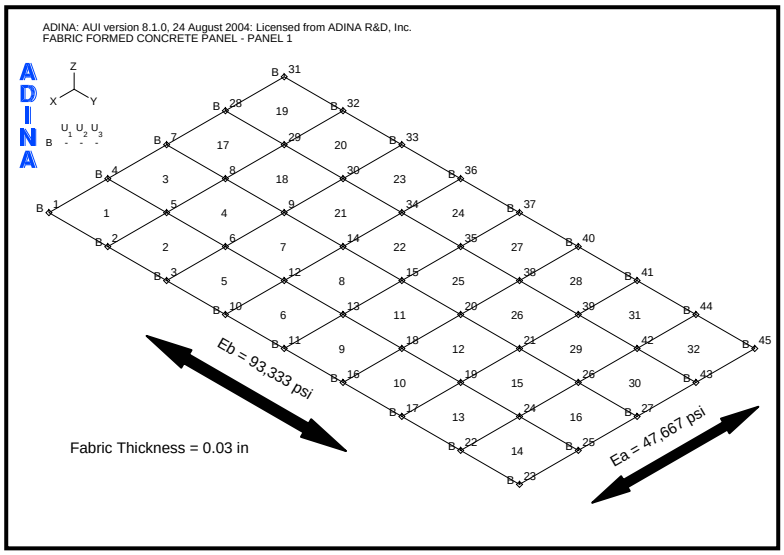

Figure 2. Panel 1 Model.

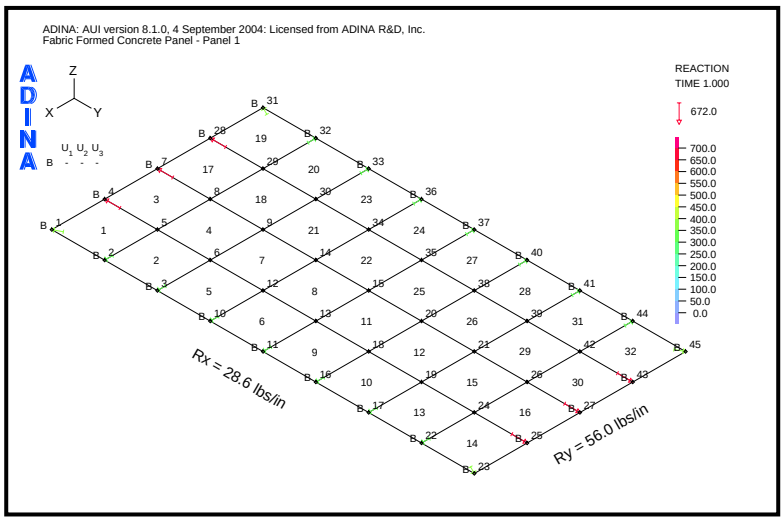

Figure 3. Panel 1 Model – Boundary Reactions.

3.3 The Combined Fabric and Slurry Model

3.3.1 Material Properties of Slurry

The slurry material, as stated above, must not contribute stiffness to the fabric element portion of the computer model. As a result, a very low Modulus of Elasticity must be used for this *elastic-isotropic* material. The slurry material will function as a load on the fabric element model using the slurry's density as a mass-proportional load. Table 2 summarizes

the slurry material properties used in the ADINA material model.

Table 2. Slurry Material Properties.

t = ***varies*** in	Slurry thickness
E = 2 psi	Modulus of Elasticity
$\nu_{sm} = 0.0$	Poisson's Ratio
$wt_{sm} = 145$ lbs/ft^3	Weight
$D_{sm} = 0.00021716366$ lb-sec^2/in^4	Density

3.3.2 ADINA Model Panel 2

Panel 2 in the ADINA model represents the supporting fabric formwork in combination with the slurry material which functions as the load on the formwork. Figure 4 shows the ADINA model. For clarity the fabric and slurry element groups have been shown separately.

The 2-D Solid fabric elements are prestressed 2% in each direction and use a large displacement/small strain Kinematic Formulation. To be consistent with the 2-D fabric elements the 3-D Solid slurry elements also use the large displacement/small strain Kinematic Formulation.

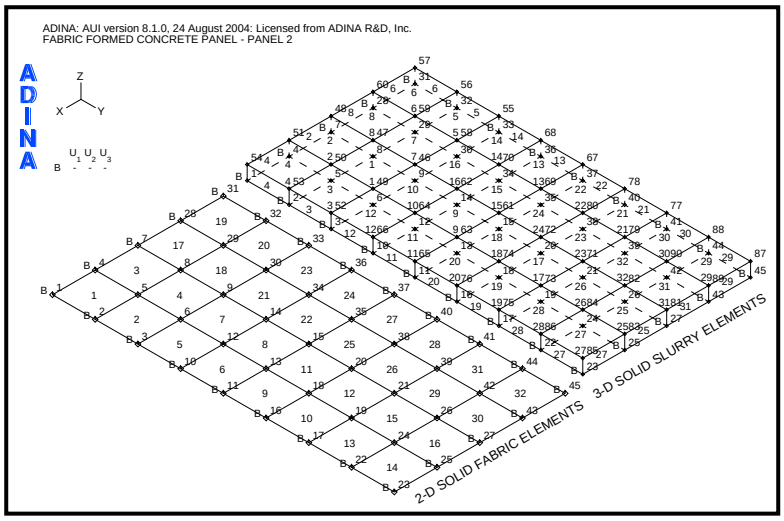

Figure 4. Panel 2 Model – Combined Fabric and Slurry Model.

Now that the model has been defined, "form-finding" of the panel shape may proceed. Initially, the 3-D slurry elements are a uniform 4" thick. The "form-finding" procedure will be as follows:

1. Run the model and determine interior fabric node displacements.
2. Increase the 3-D element thicknesses at each interior node by the amount the fabric displaces. The bottom node remains stationary while the top node is adjusted upward. (The panel is formed in reverse of how it would occur if the slurry were actually poured onto the fabric formwork.)
3. Rerun the model and determine interior fabric node displacements.
4. Repeat Steps 2-3 until displacements between last two runs are within a tolerance of approximately 1%.

After 5 iterations the final shape of Panel 2 is as shown in Figure 5. To check whether the "form-finding" procedure used to find the shape of Panel 2 is acceptable, a check using a "control" model will be performed as described in Section 3.4.

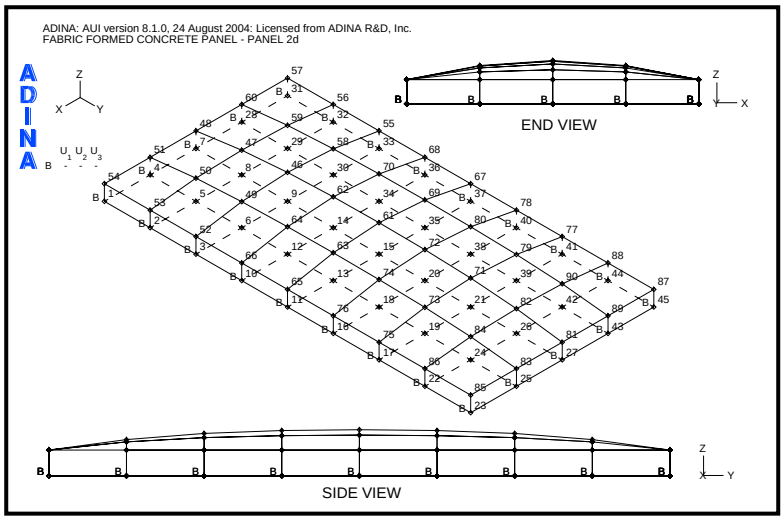

Figure 5. Panel 2 Model – Final Panel Shape.

3.4 The Control Model

Verification of Panel 2's final panel shape will be made by using a surface load spatial function applied to Panel 1. Figure 6 shows how the ADINA quadratic surface spatial function allows surface loads over an element to be varied at each node [16].

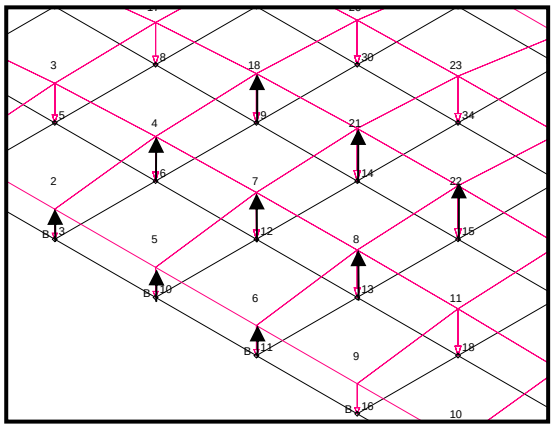

Figure 6. Quadratic Surface Spatial Function.

3.4.1 “Form-finding” Procedures

The initial uniform surface load is the equivalent of a 4” thickness of concrete. The “form-finding” procedure will be as follows:

1. Run the model and determine interior fabric node displacements.
2. Increase the surface spatial function load factors at each interior node based on density of the load required to make up these displacements.
3. Rerun the model and determine interior fabric node displacements.
4. Repeat Steps 2-3 until displacements between last two runs are within a tolerance of approximately 1%.

After 5 iterations the final shape of Panel 1, defined by the shape of the surface spatial function, is as shown in Figure 7. Table 3 gives a comparison of selected nodal displacements, maximum fabric stresses and total panel weights for each model. Figure 8 identifies the centerline nodes used for comparison purposes.

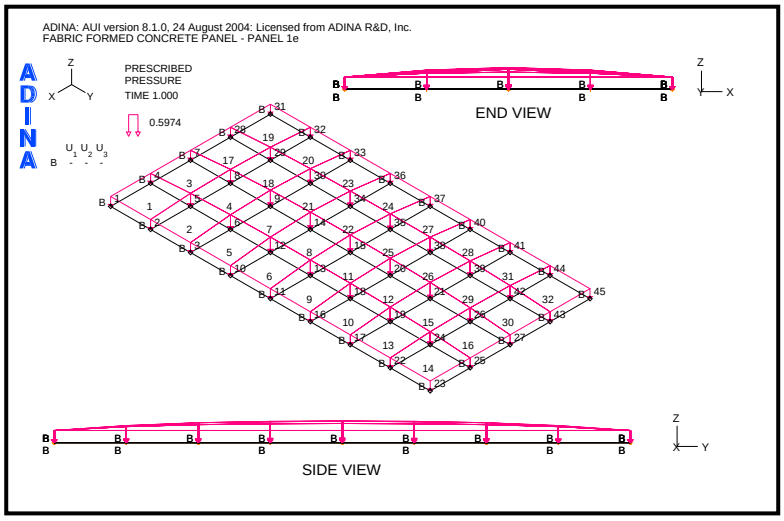

Figure 7. Panel 1 Model – Final Panel Shape.

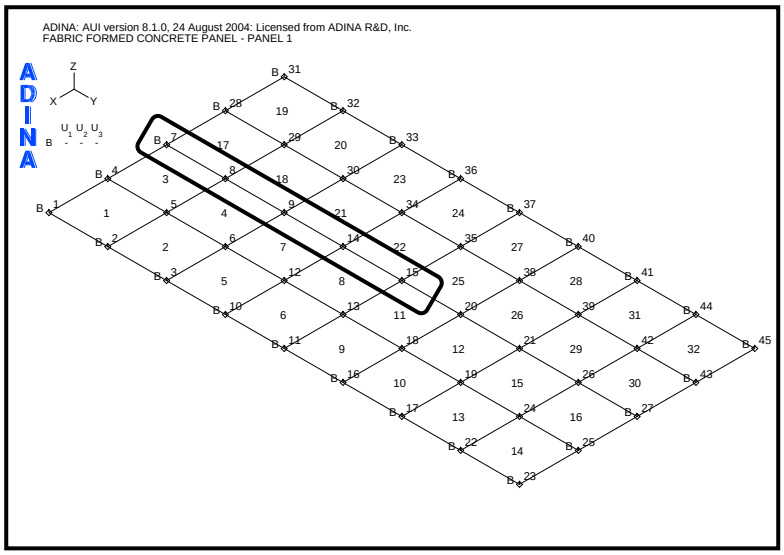

Figure 8. Fabric Model Element Nodes.

Table 3. Fabric, Model 1 and Combined Fabric and Slurry, Model 2 Iteration Results.

Iteration	1		2		3		4		5	
Panel	**1a**	**2**	**1b**	**2a**	**1c**	**2b**	**1d**	**2c**	**1e**	**2d**
Deflections (inches)										
Node 7	0.0000	0.0000	0.0000	0.0000	0.0000	0.0000	0.0000	0.0000	0.0000	0.0000
Node 8	1.2304	1.2364	1.5280	1.5339	1.5965	1.6021	1.6120	1.6175	1.6155	1.6210
Node 9	1.8951	1.9094	2.4066	2.4239	2.5264	2.5439	2.5537	2.5713	2.5599	2.5775
Node 14	2.1935	2.2106	2.8136	2.8371	2.9605	2.9853	2.9941	3.0192	3.0017	3.0269
Node 15	2.2769	2.2954	2.9284	2.9536	3.0834	3.1103	3.1188	3.1462	3.1269	3.1543
$\sigma_{y,max}$ (psi)	2068	2076	2180	2192	2209	2222	2216	2229	2218	2231
$\sigma_{z,max}$ (psi)	1236	1243	1411	1422	1459	1471	1470	1482	1473	1485
Panel Wt. (lbs)	1546.67	1547.10	1944.71	1944.95	2046.77	2046.97	2070.57	2070.82	2075.99	2076.26

Note: Percent difference in values for Panel 1e and 2d for deflections and stresses are less than 0.9%, for panel weights the difference is less than 0.02%.

3.5 Panel Designs and Optimization

Several design approaches to a fabric-formed concrete panel may be considered. Each approach must take into account the panel's final anchor locations to the backup framing system. One approach might be to locate the anchor points based on the most efficient panel design. Another may be to locate the anchor points based on the most pleasing appearance the panel takes due to the deformed fabric shape. Still another might consider both efficiency and appearance. The variables which may be subject to adjustment in the optimization process are:

- Concrete strength
- Initial panel thickness
- Prestress in fabric formwork and
- Anchor locations

With the fabric formwork modeling techniques defined, the four-step procedure outlined above may now be used to design a fabric-formed concrete panel. For demonstration purposes a 4' wide x 8' long x 2" thick panel, formed over a fabric formwork prestressed to 1%, will be designed for self-weight and a ±30 psf wind load using a concrete strength of 4,000 psi. A minimum 2" panel thickness was chosen to allow for adequate reinforcement cover, should it be required later in the design process. An initial prestress in the fabric formwork of 1% will allow for discernible fabric displacement when interior supports are used.

An optimum panel design requires that the first step be to determine the load paths the lateral loads will take to the boundary supports. The anchors are then placed at these

optimum locations anchoring the panel to the backup framing system. If, for architectural reasons, the panel was to be configured with predetermined load paths this step could be omitted.

3.5.1 Step 1 – Determination of Load Paths

A study of a 4'-0" x 8'-0" x 2" thick panel with various boundary conditions was made in order to determine the load paths the lateral load might take. A distributed unit load was applied to a series of panels and an examination of the principal stresses, for the 3-D Solid elements, was made. Figure 9 shows the boundary conditions considered and the results of these panel investigations. The general direction the maximum principal stresses took is indicated by the double headed arrows. Details of the load path study are shown in the figures of Appendix B.

Note in Figure 9 that panel anchor locations appear to result in load paths which fall into one of two cases. In Case 1, the load paths are parallel to one of the panel's edges as shown in Panel 3, which has continuous support, or Panel 3d and Panel 3g, which have symmetrical 4-point anchor locations. In Case 2, the load paths appear to triangulate and are directed between the anchor locations. These two cases will be considered when the fabric formwork is laid out and the interior and perimeter boundary conditions are introduced.

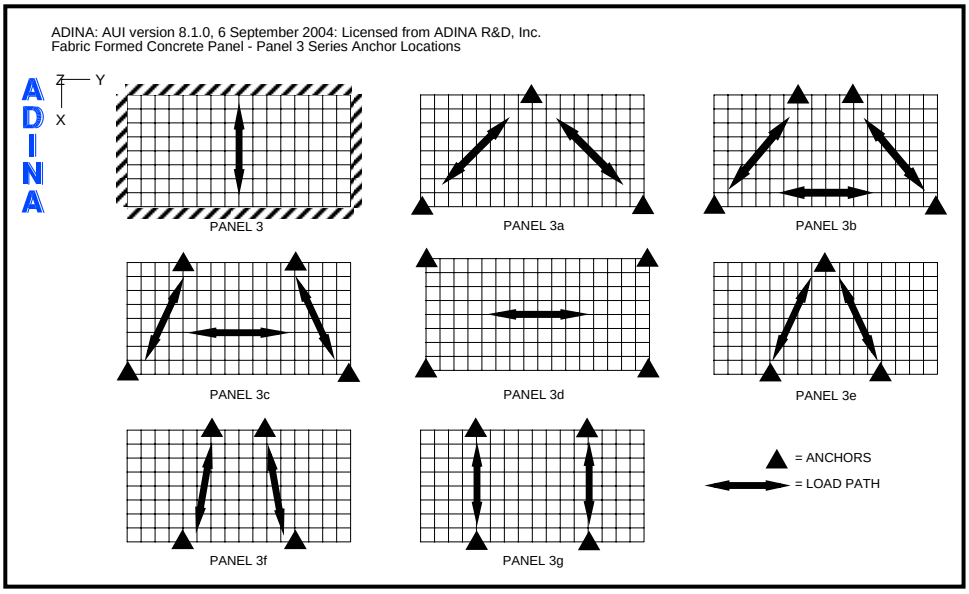

Figure 9. Panel Load Paths and Boundary Conditions.

3.5.2 Step 2 – Define Fabric Formwork Designs

Based on the study of the load paths shown in Figure 9 three fabric formwork designs were considered. Figures 10, 11 and 12 show these fabric formwork designs. Interior supports are indicated by a **"B"** in these figures. The fabric will deflect between these interior supports creating a thicker panel region – capable of resisting more load than the supported regions. These deflected regions form the "spine" of the panel and define its load paths.

Panel 4's fabric formwork, shown in Figure 10, will provide increased strength spanning the width of the panel for a continuous support condition along the length of the panel. It is modeled with one-hundred-twenty-eight 2-D Solid fabric elements. Panel 5's fabric formwork, shown in Figure 11, will provide increased strength spanning the width of the panel along a diagonal path for a 4-point anchor condition. In addition, "collector" paths are formed along the length of the panel to bring the load to the diagonal load paths. Panel 6's fabric formwork, shown in Figure 12, is similar to Panel 5 except no "collector"

paths are created. Regions between the diagonal load paths of Panel 6 may have adequate strength using the minimum panel thickness of 2". Panel 5 and 6 required three-hundred-forty-four 2-D solid fabric elements to model their formwork.

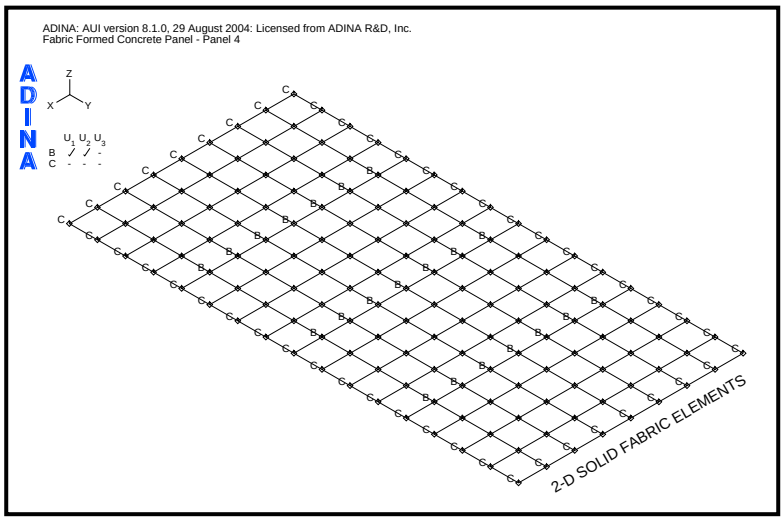

Figure 10. Panel 4 – Fabric Formwork Design.

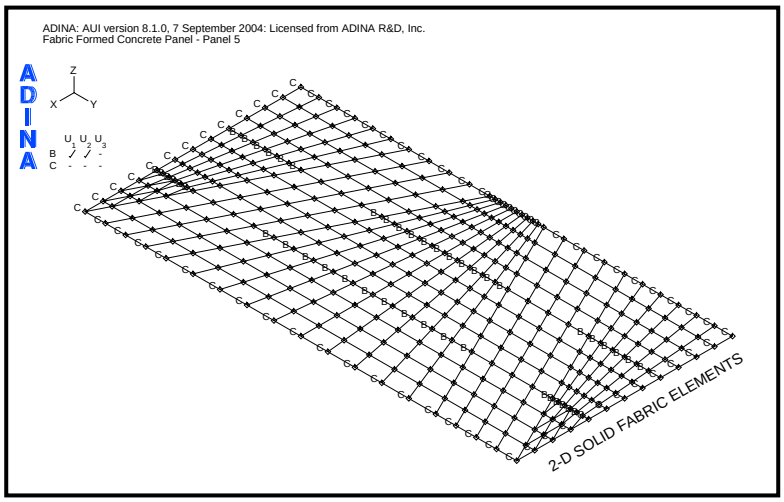

Figure 11. Panel 5 – Fabric Formwork Design.

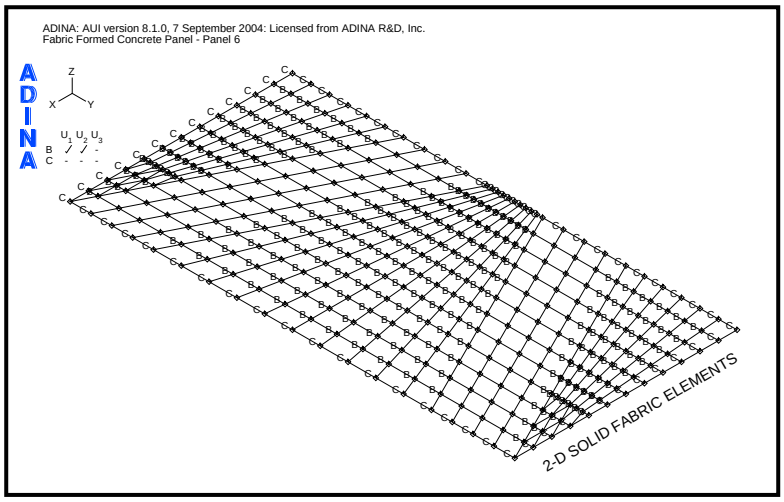

Figure 12. Panel 6 – Fabric Formwork Design.

3.5.3 Step 3 – "Form-finding" Panel Shapes

The results of "form-finding" the panel shapes for Panels 4, 5 and 6, given the initial design conditions noted above, are shown in Figures 13, 14 and 15, respectively. These finite element models show the initial panel shapes made up of the slurry material. One-hundred-twenty-eight, 8-node, 3-D Solid slurry elements are used to model Panel 4. Three-hundred-forty-four, 8-node, 3-D Solid slurry elements were required for Panels 5 and 6. The boundary conditions which created them were illustrated in Figures 10, 11 and 12, respectively.

A strength analysis of the panels will need to be performed before any judgment of which panel shape is most efficient can be made. Individual panel designs may be optimized, to account for over or under-strength, by adjusting the variables noted above and repeating Steps 3 and 4 of the design procedure.

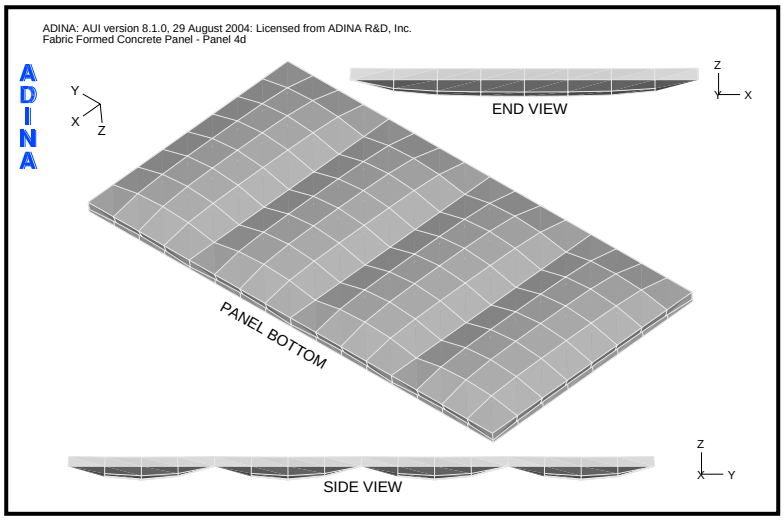

Figure 13. Panel 4 – Initial Panel Shape.

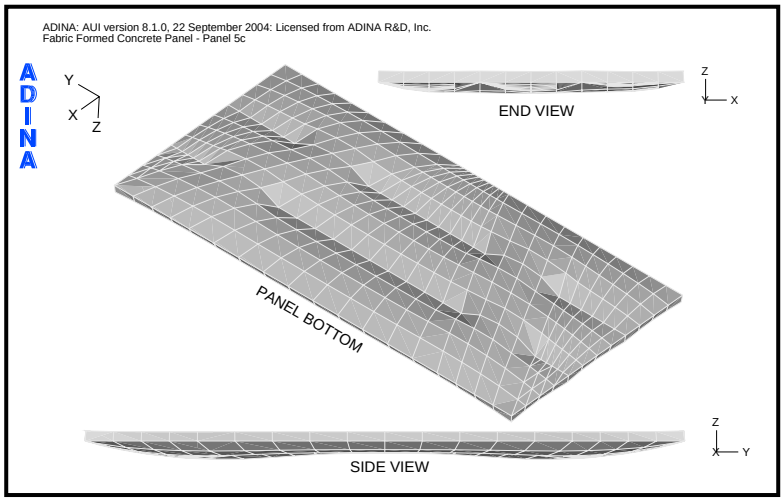

Figure 14. Panel 5 – Initial Panel Shape.

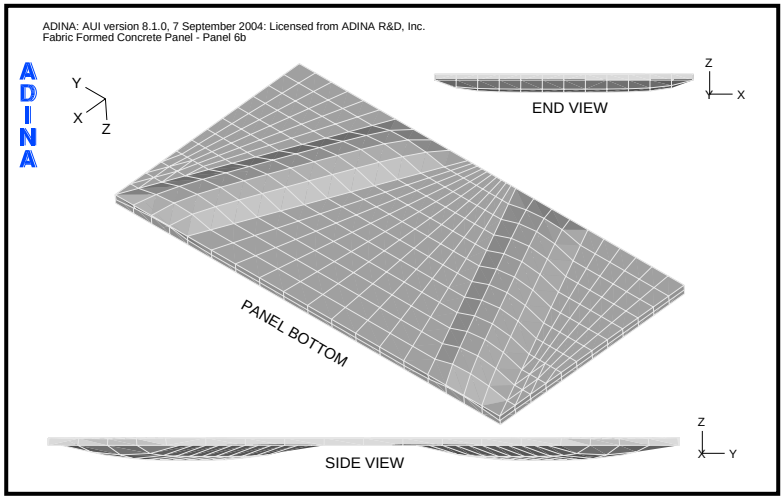

Figure 15. Panel 6 – Initial Panel Shape.

3.6 Panel Loads and Materials

3.6.1 Design Loads

The initial panel shapes defined in Figures 13, 14 and 15 may now be analyzed for strength under the ±30 psf design lateral wind load and gravity self weight. The lateral loads will act to cause bending in the panel and the gravity loads are in-plane loads which will contribute to membrane action in the vertically oriented panel. Two lateral load cases are considered; a positive load case and a negative load case. See Figure 16. The panels will be analyzed using the strength design method for plain concrete and ACI 318-02 Section 22 [19]. The required factored loads are

$$P_D = 1.2 \times D_c\,, \tag{4}$$

$$P_W = 1.6 \times 30 \text{ psf} = 48 \text{ psf} \tag{5}$$

where

D_c Density of concrete panel,

P_D Factored dead load,

P_W Factored wind load.

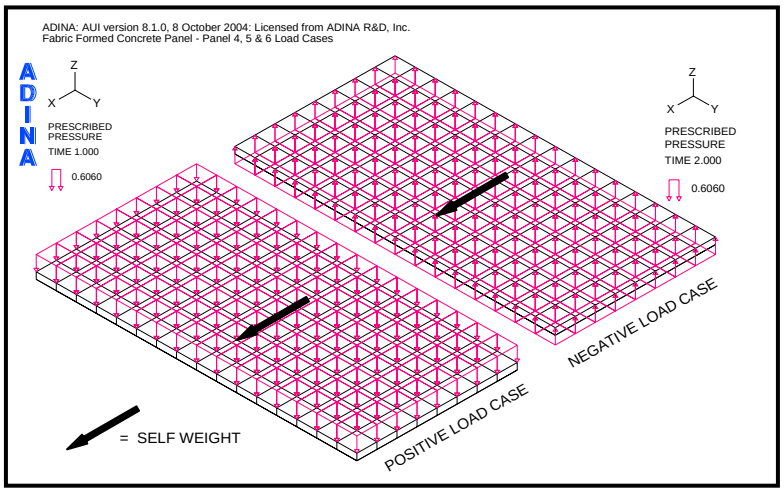

Figure 16. Panel Load Cases.

3.6.2 Material Properties

The properties for the slurry material are now replaced with the properties for concrete. Table 4 summarizes the concrete material properties used in the ADINA material model.

Table 4. Concrete Material Properties.

t = ***varies*** in	Concrete panel thickness
E_c = 3,644,147 psi	Secant Modulus of Elasticity
E_{tc} = 6,377,258 psi	Initial Tangent Modulus of Elasticity (Assume 1.75 x Secant Modulus)
D_c = 0.00021716366 lb-sec^2/in^4	Density of concrete
f'_c = 4,000 psi	Compressive strength of concrete (SIGMAC)
ε_c = 0.002	Compressive strain of concrete at SIGMAC
f'_{uc} = 3,400 psi	Ultimate compressive strength of concrete (SIGMAU, assumed @ 85% f'_c)
ε_{uc} = 0.003	Ultimate compressive strain of concrete at SIGMAU
$f_r = 5\sqrt{f'_c}$ = 316.2 psi	Uniaxial cut-off tensile strength of concrete
ν_c = 0.20	Poisson's Ratio
wt_c = 145 lbs/ft^3	Weight
Φ_p = 0.55	Strength reduction factor for plain concrete

Where the panel is reinforced, model material properties for the reinforcing steel are summarized in Table 5.

Table 5. Reinforcing Steel Material Properties.

E_s = 29,000,000 psi	Young's Modulus of Elasticity
E_{ts} = 290,000 psi	Strain hardening (Tangent) Modulus
D_s = 0.0007339 lb-sec^2/in^4	Density of steel
f_y = 60,000 psi	Initial yield stress

Stress-strain curves for the concrete and reinforcing steel are shown in Figures 17 and 18, respectively.

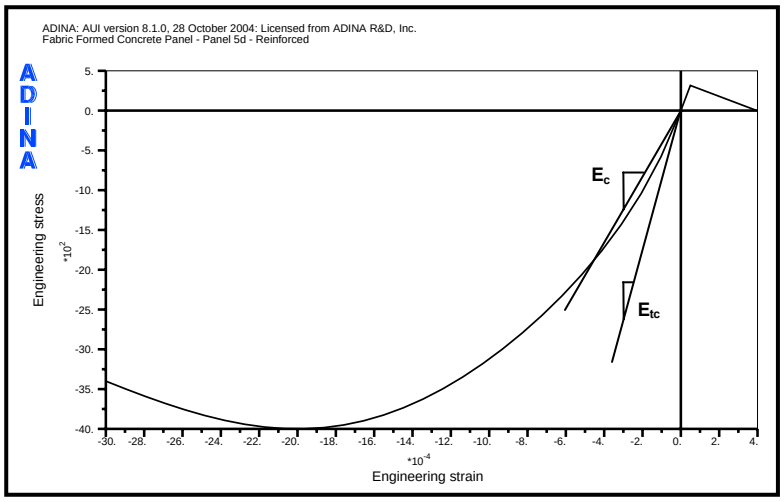

Figure 17. Stress-strain Curves for Concrete.

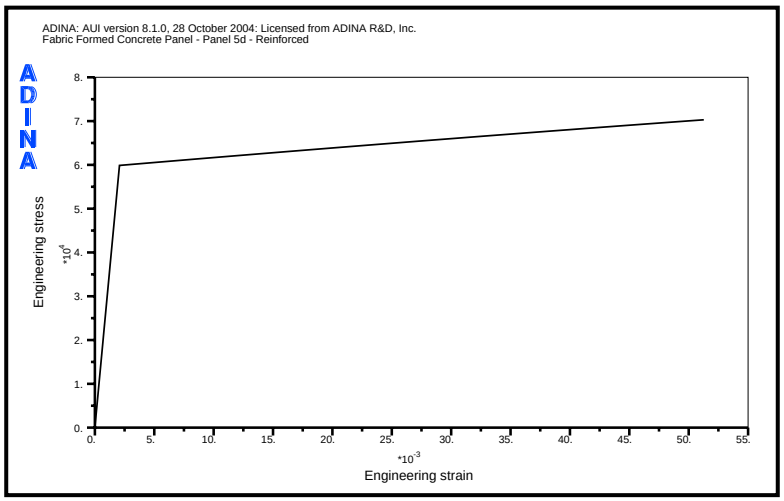

Figure 18. Stress-strain Curves for Reinforcing Steel.

Panel analysis was carried out using the structural analysis program ADINA. The panels were designed using structural plain concrete design criteria. The governing criteria for plain concrete design is the uniaxial cut-off strength of the concrete or Modulus of Rupture. Maximum principal tensile stresses resulting from positive and negative wind loads combined with gravity loads must fall below this value. When the maximum principal tensile stress is greater than the Modulus of Rupture the ADINA model indicates this point by a "crack" in the panel model. The ADINA Theory and Modeling Guide notes: "…for

concrete…. these are true principal stresses only before cracking has occurred. After cracking, the directions are fixed corresponding to the crack directions and these variables are no longer principal stresses" [15]. Following are summary graphic output for the three panel types under investigation.

SECTION 4 – STEP 4 - PANEL DESIGN AND DISCUSSION

4.1 Panel 4 – Analysis and Design

Figure 19 shows the FEA model for Panel 4 and its factored lateral load. Positive and negative load cases were considered. See Figure 16. The finite elements are arranged in a regular pattern and are simply supported along the length of the model. The panel had a final weight of 857.8 lbs after the first design configuration. Figures 20 and 21 show the loading conditions under which the panel first cracks. For both of these cases the first cracks are initiated at loads well in excess of the required factored load. It is possible to optimize this panel by adjusting one or more of the design variables outlined in Section 3.5.

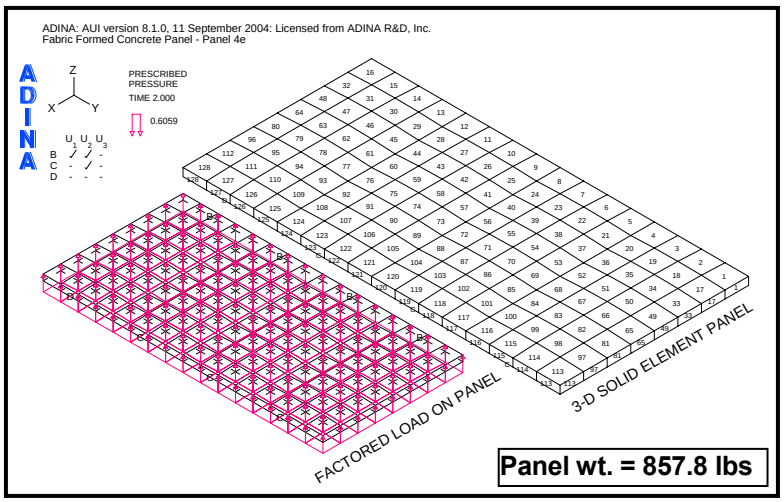

Figure 19. Panel 4 – Model, Configuration 1.

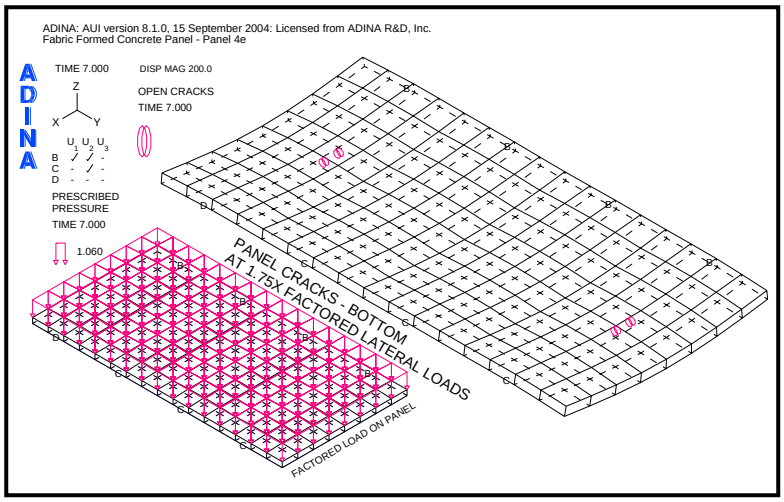

Figure 20. Panel 4 – First Cracks, Panel Bottom, Configuration 1.

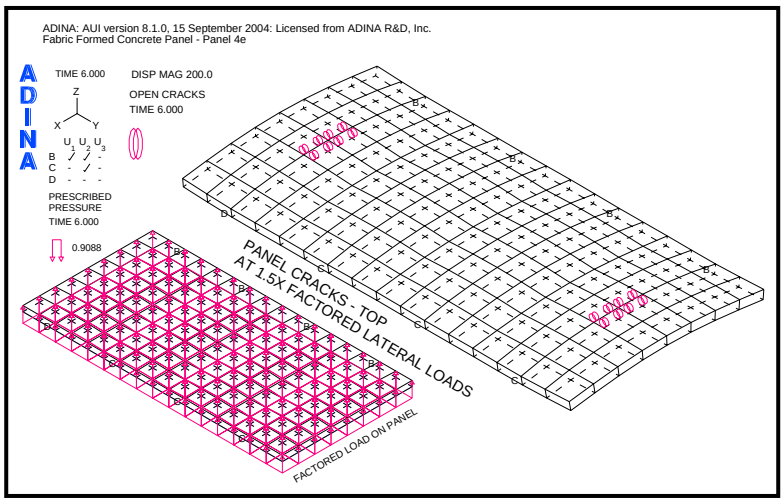

Figure 21. Panel 4 – First Cracks, Panel Top, Configuration 1.

A second design configuration using a fabric prestress of 2% along the length of the panel and 1% along its width, to reduce the amount of concrete required, was carried out. Results of this second design configuration are shown in Figures 22 and 23. From these figures it is clear that the panel still has excess capacity and is not of an optimal form.

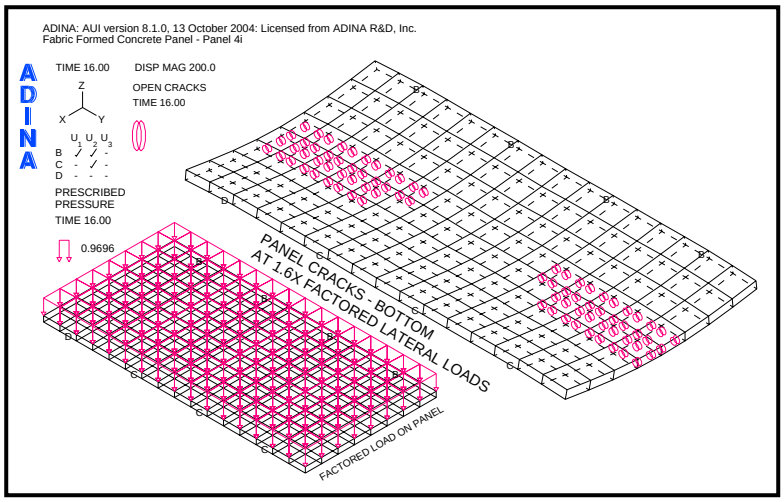

Figure 22. Panel 4 – First Cracks, Panel Bottom, Configuration 2.

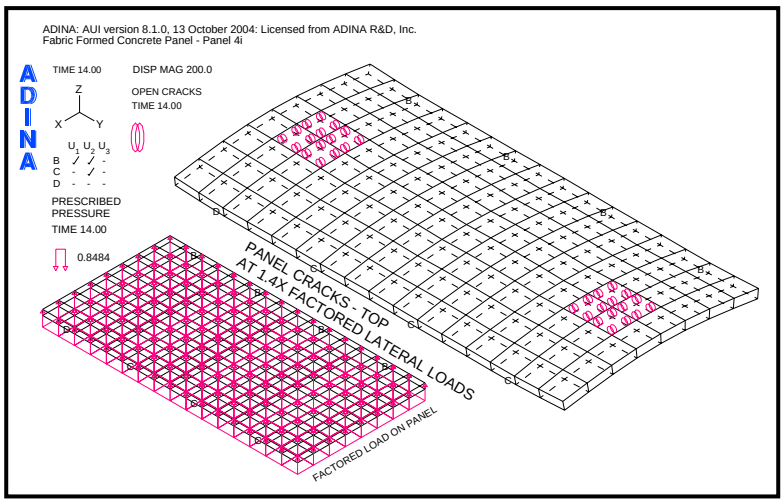

Figure 23. Panel 4 – First Cracks, Panel Top, Configuration 2.

The decision was made to check the panel with a uniform thickness of 2" and without the use of the fabric formwork. This design configuration amounts to the trivial solution, but it requires checking. Figure 24 shows the FEA model and its factored lateral load. The panel had a final weight of 773.3 lbs after this third design configuration. Figure 25 shows the deflected shape under the positive load case. Figures 26 and 27 show the loading conditions under which the panel first cracks. For both of these cases, the first cracks are initiated at loads in excess of the required factored load. The optimal form for this simply

supported panel was found to be one with a uniform thickness of 2".

To observe how the crack patterns form for an overload condition the crack patterns at 1.9 times the factored load cases are shown in Appendix C, Figures C1 and C2. Figures 28 and 29 show the maximum principal tensile stresses for the two loading conditions at the factored load. The load path between the supports is indicated by the double-headed arrow which follows the general direction the maximum principal stresses take. This corresponds to the load path for Panel 3g shown in Figure 9.

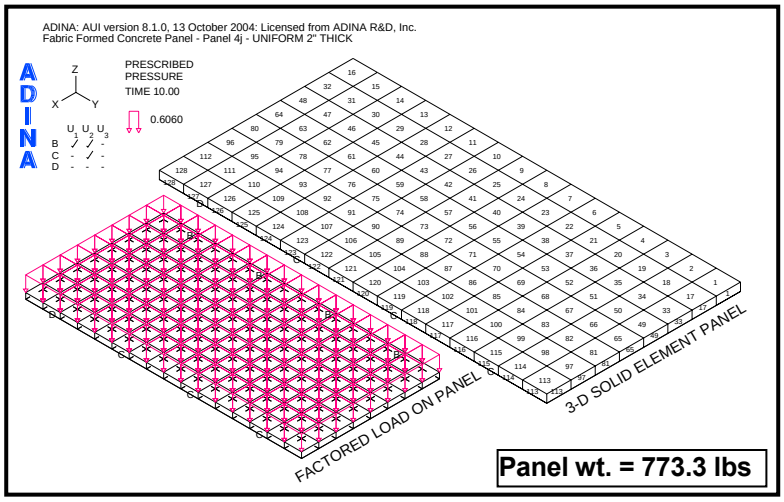

Figure 24. Panel 4 – Model, Configuration 3.

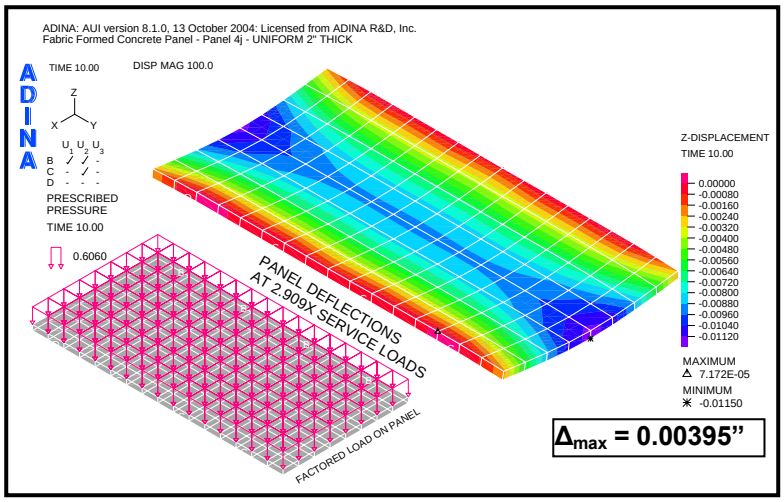

Figure 25. Panel 4 – Deflections, Configuration 3.

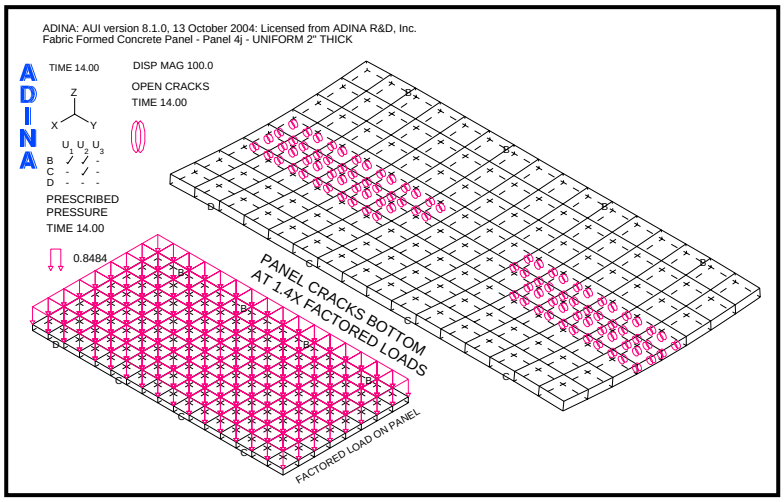

Figure 26. Panel 4 – First Cracks, Panel Bottom, Configuration 3.

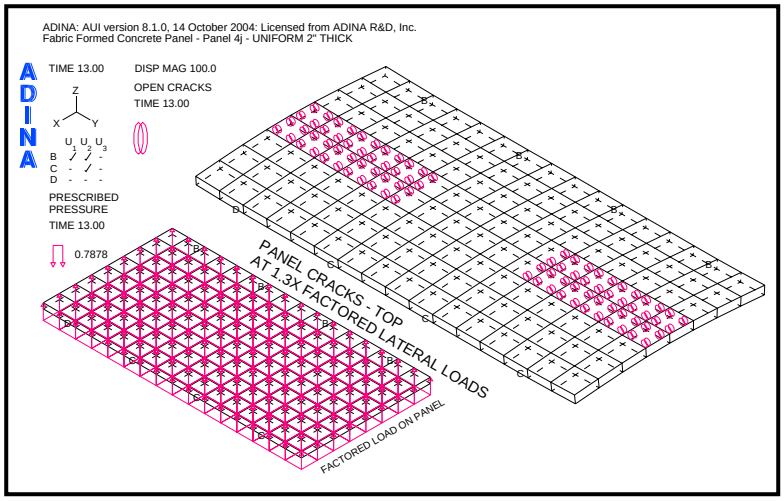

Figure 27. Panel 4 – First Cracks, Panel Top, Configuration 3.

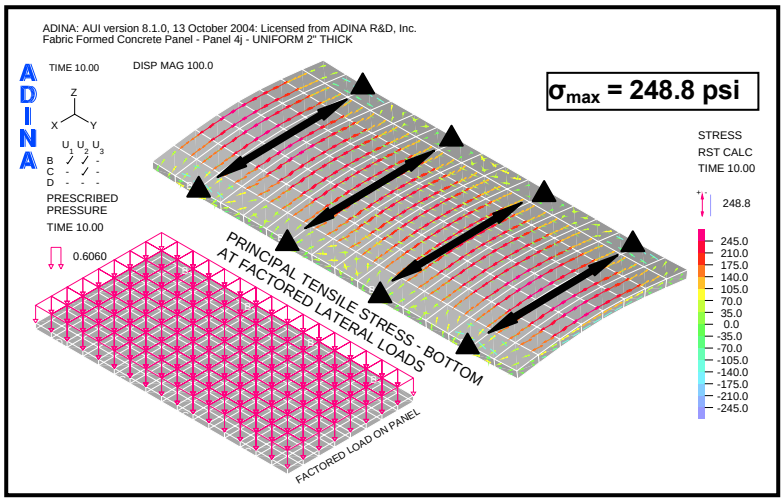

Figure 28. Panel 4 – Principal Stresses, Panel Bottom, Configuration 3.

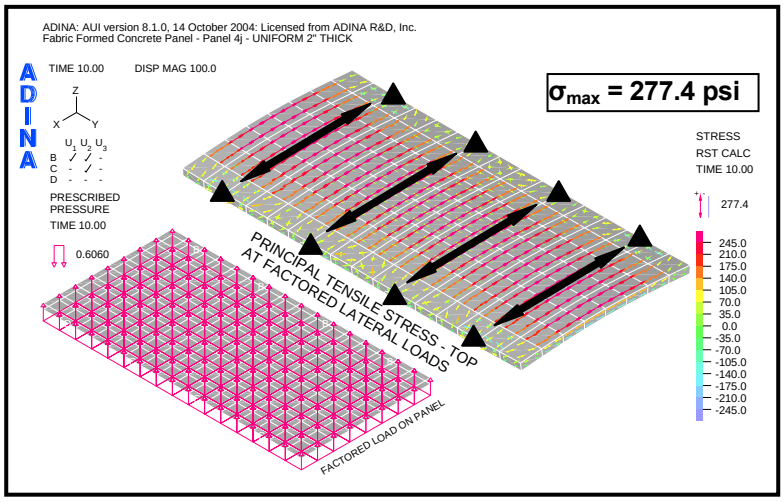

Figure 29. Panel 4 – Principal Stresses, Panel Top, Configuration 3.

4.2 Panel 5 – Analysis and Design

Figure 30 shows the FEA model for Panel 5 and its factored lateral load. Positive and negative load cases were considered. See Figure 16. The finite elements are arranged in a pattern that follows the fabric formwork design shown in Figure 11 and are supported with a 4-point anchor arrangement. The panel had a final weight of 881.3 lbs. Figure 31 shows the deflected shape under the positive load case. Figures 32 and 33 show the loading conditions under which the panel first cracks. For case one first panel cracks are initiated at 1.1 times the factored loads. For case two the first cracks occur when the required factored

load case is reached. To observe how the crack patterns form for an overload condition the crack patterns at 1.5 times the factored load cases are shown in Appendix C, Figures C3 and C4. Figure 34 shows the maximum principal *tensile* stresses for the positive lateral load case at the factored load. Figure 35 shows the maximum principal *tensile* stresses for the negative lateral load case at 0.9 times the factored load. The load path between the supports is indicated by the double-headed arrow. This corresponds to the load path for Panel 3b shown in Figure 9. This panel has an equivalent uniform thickness of 2.28", has achieved an optimal form and its final panel shape remains the same as the initial shape shown in Figure 14.

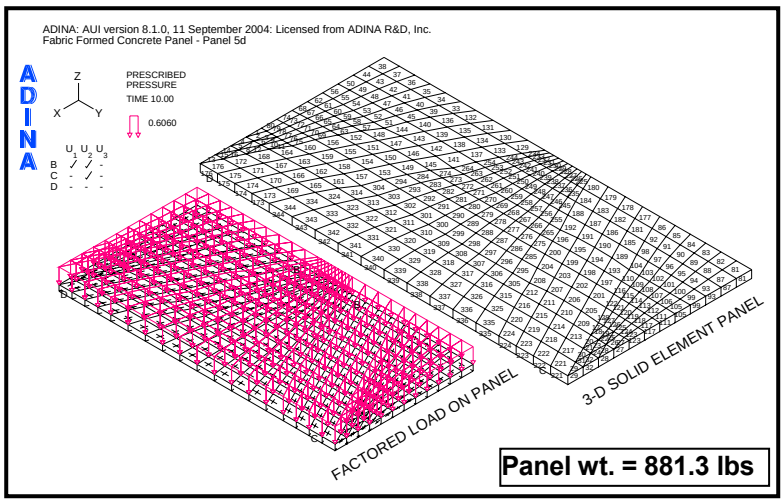

Figure 30. Panel 5 – Model.

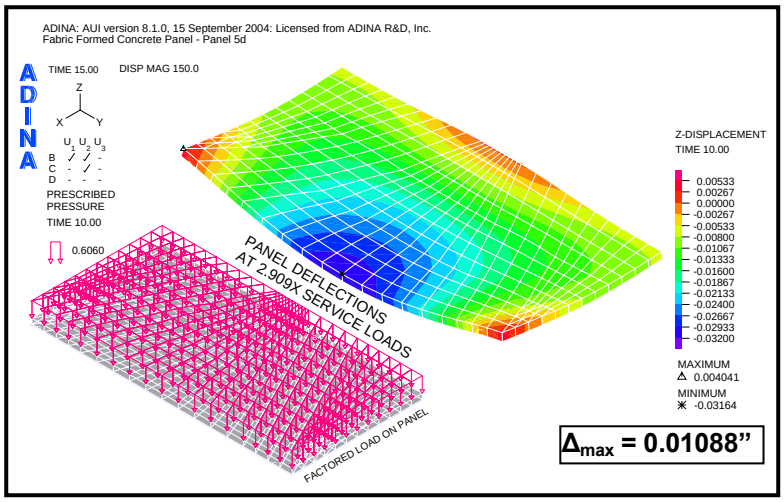

Figure 31. Panel 5 – Deflections.

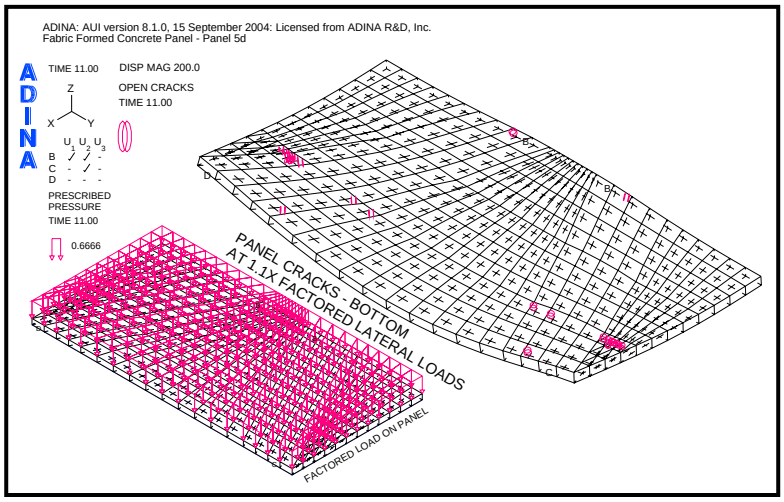

Figure 32. Panel 5 – First Cracks, Panel Bottom.

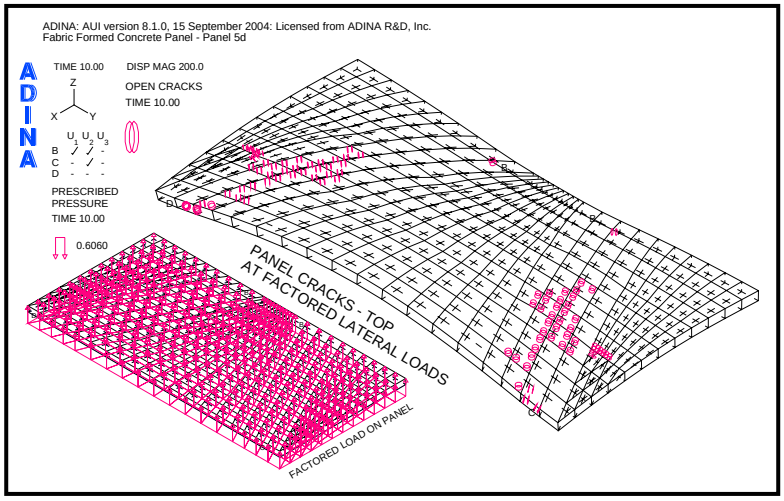

Figure 33. Panel 5 – First Cracks, Panel Top.

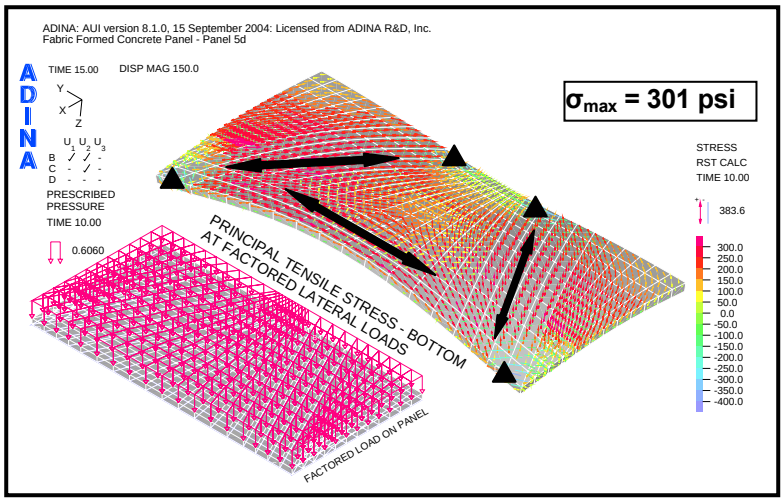

Figure 34. Panel 5 – Principal Stresses, Panel Bottom.

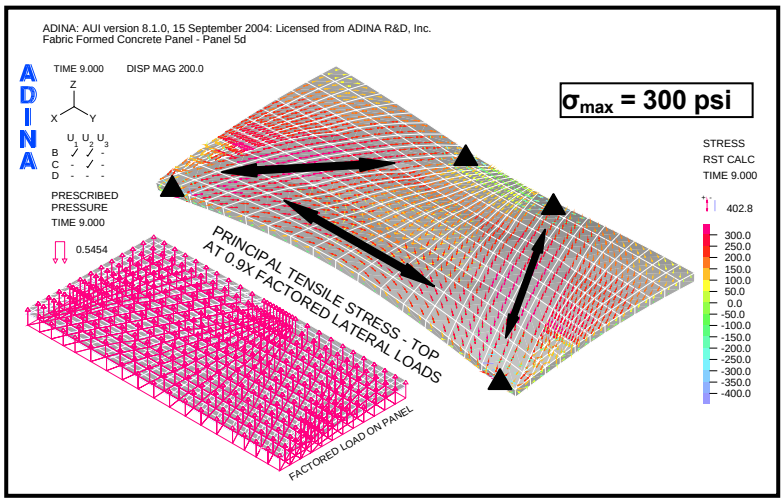

Figure 35. Panel 5 – Principal Stresses, Panel Top.

4.3 Panel 6 – Analysis and Design

Figure 36 shows the FEA model for Panel 6 and its factored lateral load. This panel design also considered positive and negative load cases. See Figure 16. The finite elements are arranged in a pattern that follows the fabric formwork design shown in Figure 12 and are supported with a 4-point anchor arrangement. The panel had a final weight of 790.3 lbs after the first design configuration. Figures 37 and 38 show the loading conditions under which the panel first cracks. For case one first panel cracks are initiated at 0.9 times the

factored loads. For case two the first cracks occur at 0.8 times the factored load case. This panel is "under-strength" and requires optimization. Since the initial panel cracks occur in the 2" thick portion of the panel an increase in the panel's thickness is required.

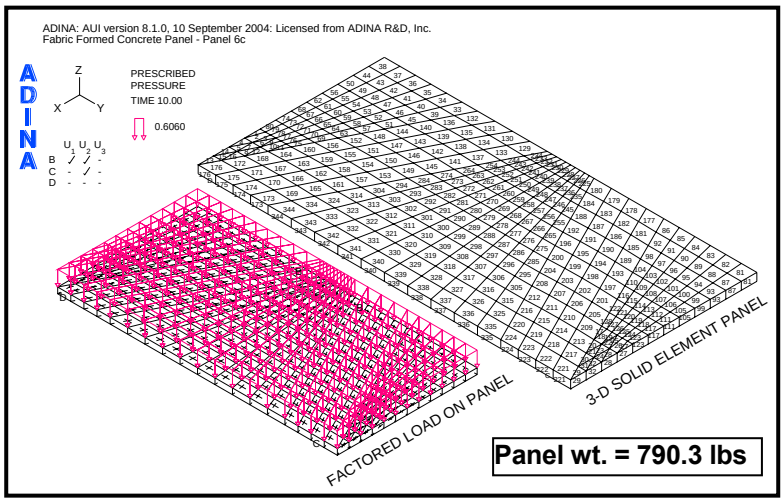

Figure 36. Panel 6 – Model, Configuration 1.

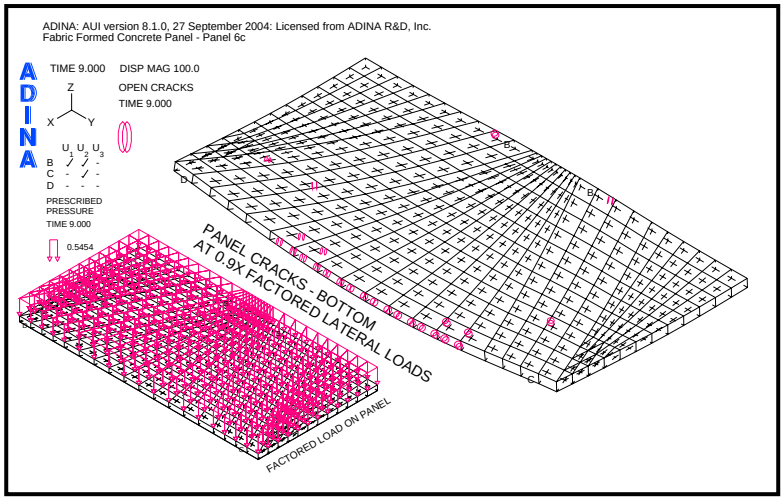

Figure 37. Panel 6 – First Cracks, Panel Bottom, Configuration 1.

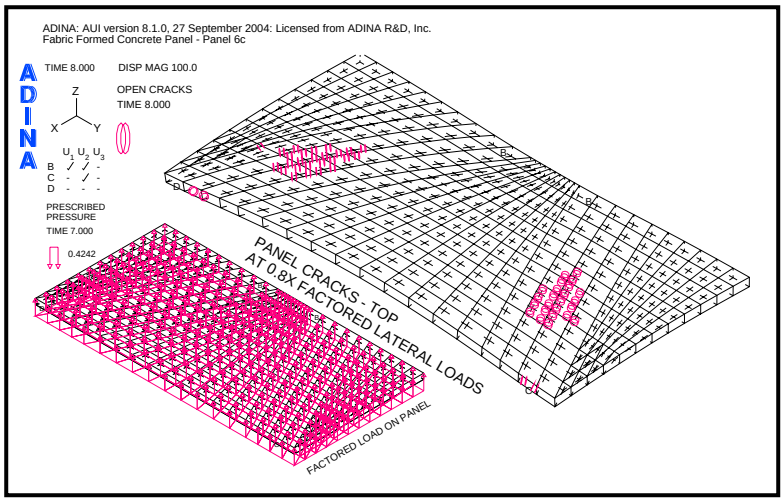

Figure 38. Panel 6 – First Cracks, Panel Top, Configuration 1.

The second design configuration uses an initial panel thickness of 3". Results of this second design configuration are shown in Figures 39 and 40. These results show the panel to have excess capacity with initial cracks occurring well over the required factored loads. A third design configuration is required.

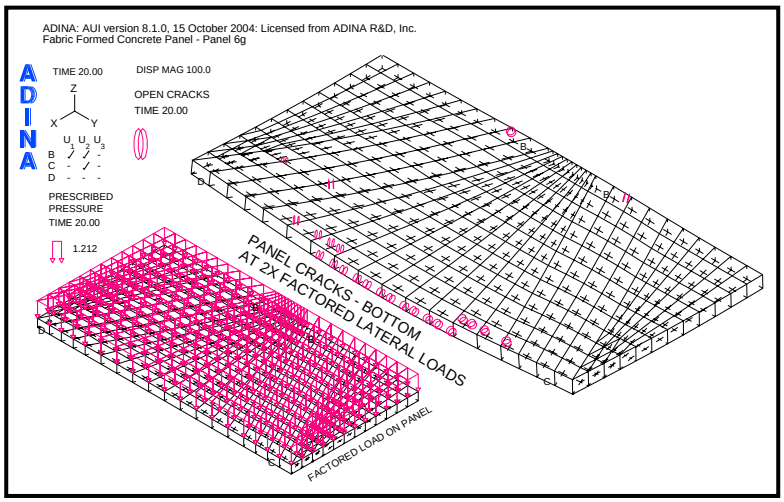

Figure 39. Panel 6 – First Cracks, Panel Bottom, Configuration 2.

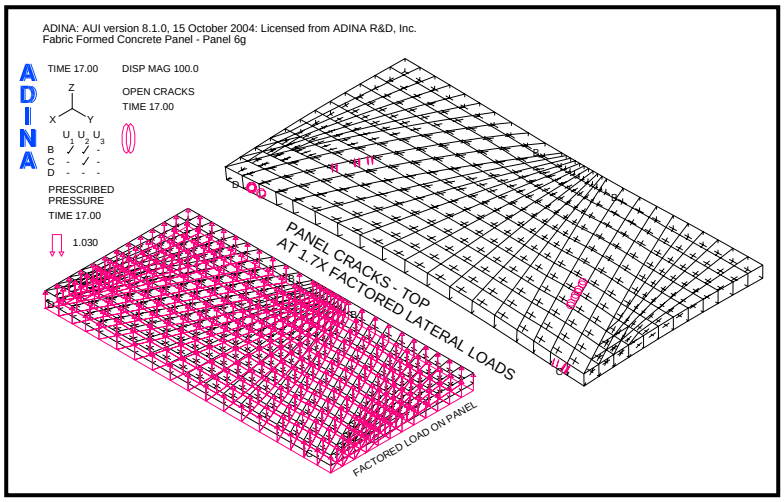

Figure 40. Panel 6 – First Cracks, Panel Top, Configuration 2.

A reduction in the panel's thickness to 2 ½" was used in a third design configuration. The results of the third design configuration are shown in Figures 41 and 42. These results show the panel to still have excess capacity with initial cracks occurring over the required factored loads. A fourth design configuration to optimize the panel is required.

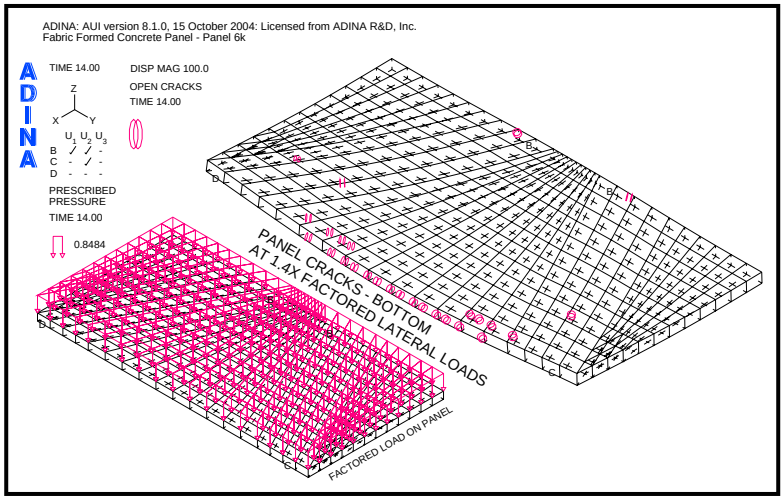

Figure 41. Panel 6 – First Cracks, Panel Bottom, Configuration 3.

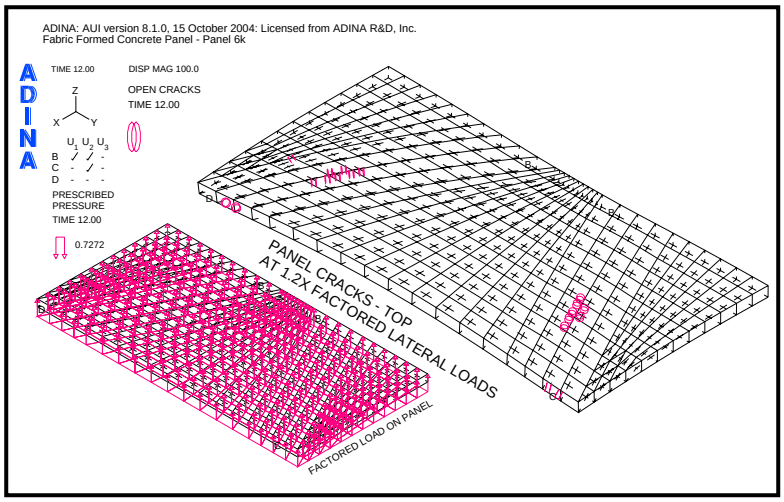

Figure 42. Panel 6 – First Cracks, Panel Top, Configuration 3.

The decision was made to check the panel with a uniform thickness of 2 ½" and without the use of the fabric formwork. This design configuration also amounts to the trivial solution. Figure 43 shows the FEA model and its factored lateral load. The panel had a final weight of 966.7 lbs after this fourth design configuration. Figure 44 shows the deflected shape under the positive load case. Figures 45 and 46 show the loading conditions under which the panel first cracks. For both of these cases the first cracks are initiated at a load in excess of the required factored load. The optimal form for this simply supported panel is found to be one with a uniform thickness of 2 ½".

To observe how the crack patterns form for an overload condition the crack patterns at 1.5 times the factored load cases are shown in Appendix C, Figures C5 and C6. Figures 47 and 48 show the maximum principal tensile stresses for the two loading conditions at the factored load. The load path between the supports is indicated by the double-headed arrow which follows the general direction the maximum principal stresses take. This corresponds to the load path for Panel 3b shown in Figure 9.

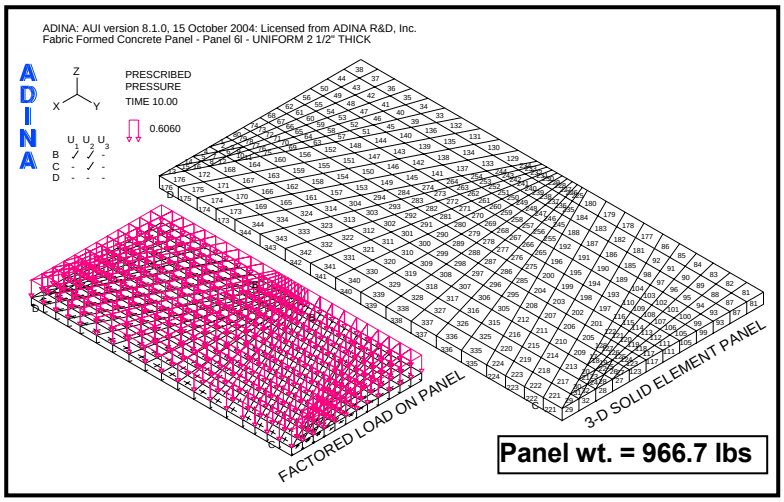

Figure 43. Panel 6 – Model, Configuration 4.

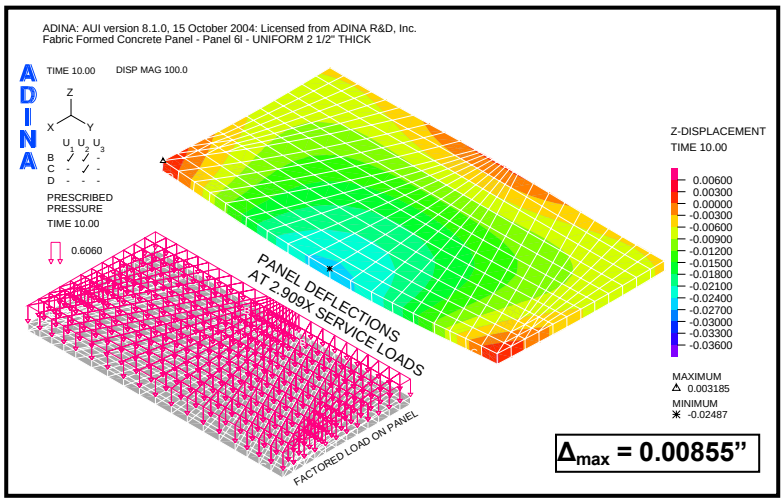

Figure 44. Panel 6 – Deflections, Configuration 4.

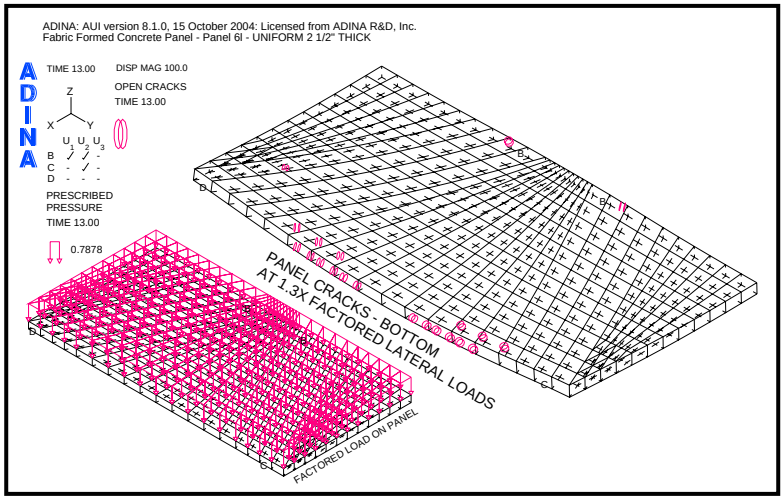

Figure 45. Panel 6 – First Cracks, Panel Bottom, Configuration 4.

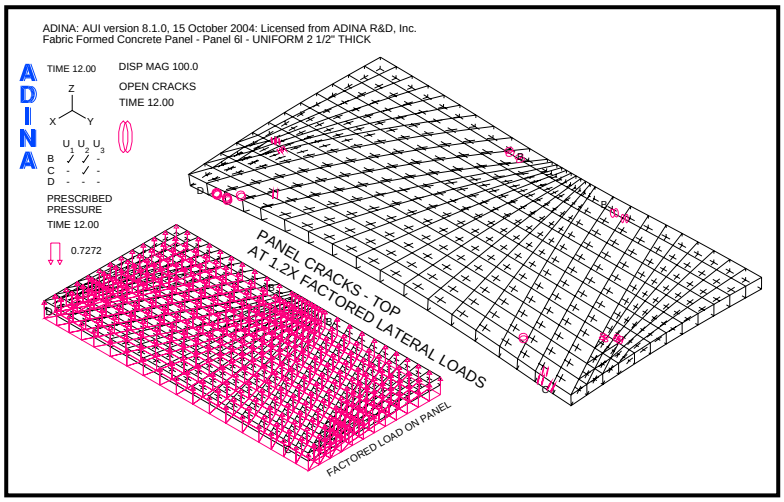

Figure 46. Panel 6 – First Cracks, Panel Top, Configuration 4.

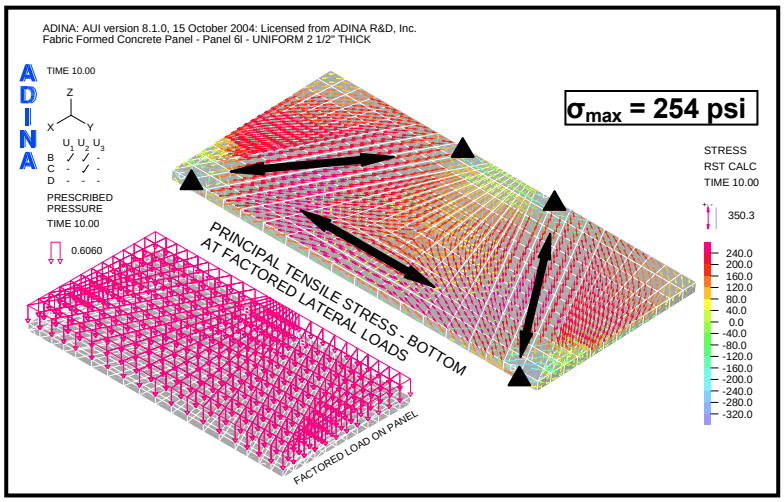

Figure 47. Panel 6 – Principal Stresses, Panel Bottom, Configuration 4.

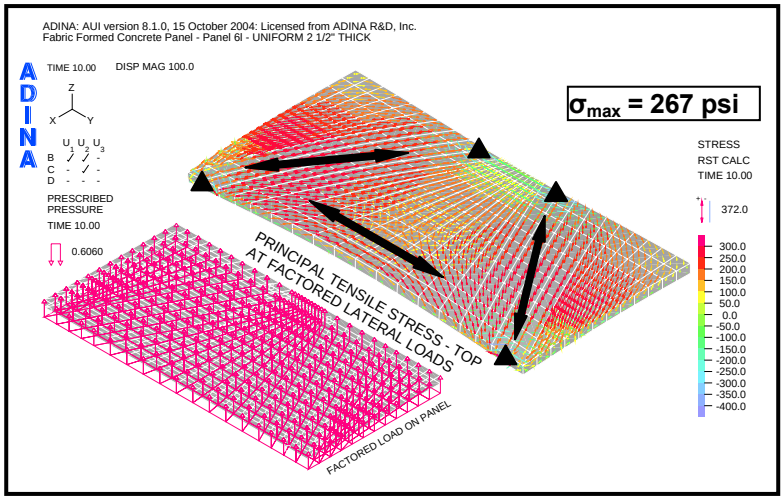

Figure 48. Panel 6 – Principal Stresses, Panel Top, Configuration 4.

4.4 Reinforcement Considerations

The results of a plain concrete analysis for the three panel designs under investigation show that the optimum shape for Panels 4 and 6 is a panel with a uniform thickness. A slight increase in concrete strength, relaxation of the fabric formwork, or a reinforced design might be considered for Panel 5 which appears to be marginal as the factored load is approached, but otherwise adequate.

Panel 5 is a minimum of 2" thick and reinforcing it would require the reinforcing be placed at the center of the panel in order to maintain cover to the reinforcement. Figure 49 shows one possible reinforcement arrangement for Panel 5. The reinforcement is placed along the load paths where the principal tensile stresses are greatest.

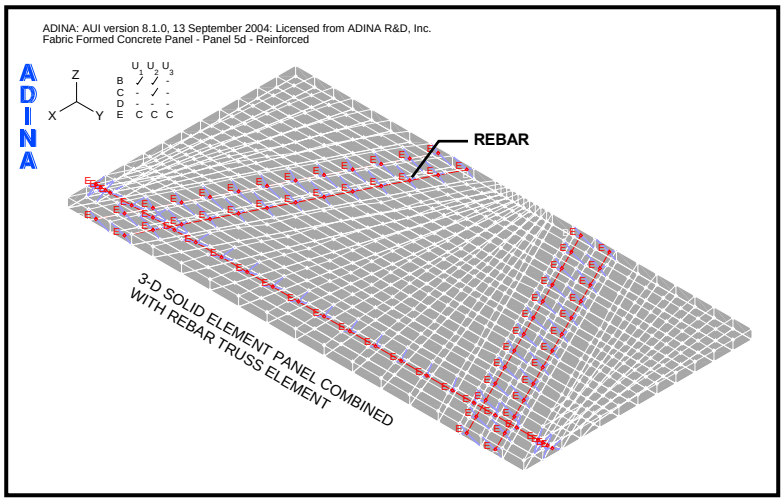

Figure 49. Panel 5 – Reinforced Model.

Analysis of Panel 5 was carried out using a reduced number of Gauss points through the thickness of the panel; three versus the six used investigating the plain concrete panels. See Figure 50. Even though reinforcing has been used, a comparison with the plain concrete panel design showed no reduction in the crack patterns for both the positive and negative wind load cases. See Appendix C Figures C7 – C10 for a comparison of these results.

If the uniformly 2" thick wall Panel 4 were to be designed as a reinforced panel the minimum amount of required reinforcement would consist of a mesh of 10 x 10 – D4 x D4 welded wire fabric placed at the center of the panel.

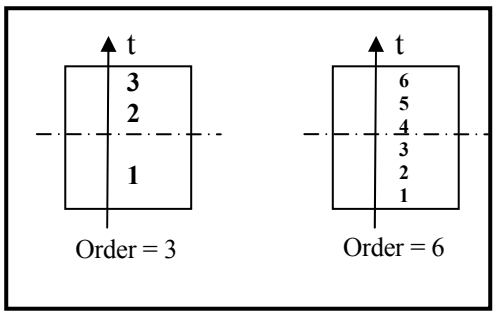

Figure 50. Gauss Integration in the Element Thickness Direction.

SECTION 5 – CONCLUSIONS AND RECOMMENDATIONS

5.1 Conclusions

The procedures introduced in this report have proven useful in the analysis and design of flexible fabric formworks and the complex concrete panel shapes they formed. The slurry material used with the 3-D Solid finite element proved very useful in saving FEA modeling time by allowing the panel shape to be formed and then later analyzed by substituting a concrete material model for the slurry material model without remeshing the FEA model. Model verification using the quadratic spatial surface function to modify the unit distributed load over an element showed that good accuracy with the proposed procedures can be assured.

The computer program, ADINA, is well suited to analyze the complex shapes a fabric formed concrete panel can take. In addition, it is capable of utilizing the different material models required at each step of the design process.

A comparison of Panels 5 and 6 results in Table 6 shows the efficiency of using the fabric formwork to stiffen Panel 5 along its length by adding "collector" paths. Panel 5 is 85.4 lbs lighter than the uniformly thick Panel 6 which used the same boundary conditions.

Table 6. Panels 4, 5 and 6 Thicknesses and Weights.

Panel	**4**	**5**	**6**
Panel Thicknesses (in)	2.0	2.28 (E.U.T.)*	2.50
Panel Weight (lbs)	773.7	881.3	966.7

* E.U.T. = Equivalent Uniform Thickness.

See Appendix D for ¼-scale model photos of Panel 5.

5.2 Recommendations

The development of computer software which would automatically "form-find" the panel shape and then allow it to be analyzed is a must. Depending upon the complexity of the panel and fineness of the FEA mesh it can take three to five iterations to determine the final panel shape. Panel 5, for example, took five iterations to find its final shape. Two-hundred-forty-nine 3-D element nodes required position updating for each iteration. The hand methods employed here for updating the geometry are feasible for only small panels.

5.3 Future Research

The following list of research topics would prove useful in furthering the development of this method of forming concrete panels.

- Perform design verification by analysis and testing of full-scale wall panels for deflections and load carrying capacities for both reinforced and plain concrete.
- Investigate optimal reinforcement patterns for a given panel shape.
- Determine the role creep plays in the design process when using geotexile fabric as the flexible formwork.
- Investigate the use of fiber reinforced concrete in panel design.
- Investigate the use of flexible formworks of other material types.

REFERENCES

[1] West, Mark. October 2003. "Fabric-Formed Concrete Members." *Concrete International* Vol. 25(10), pp. 55+.

[2] West, Mark. April 2002. "Fabric-Cast Concrete Wall Panels." Materials Technology Workshop, Department of Architecture, University of Manitoba, Canada. [Internet, WWW]. *Address:* http://www.umanitoba.ca/faculties/architecture/cast/CASTonline.html; [Accessed: 11 November 2003]. A copy of this document is available from the author.

[3] West, Mark. "A Brief Description of Fabric-Formed Concrete." Department of Architecture, University of Manitoba, Canada. [Internet, WWW]. *Address:* http://www.umanitoba.ca/faculties/architecture/cast/CASTonline.html; [Accessed: 11 November 2003]. A copy of this document is available from the author.

[4] West, Mark. "Fabric-Formed Concrete Structures." Department of Architecture, University of Manitoba, Canada. [Internet, WWW]. *Address:* http://www.umanitoba.ca/faculties/architecture/cast/CASTonline.html; [Accessed: 11 November 2003]. A copy of this document is available from the author.

[5] West, Mark. "Construction-Research-Design-Invention, Elastic Behavior in a Moist Environment." Department of Architecture, University of Manitoba, Canada. [Internet, WWW]. *Address:* http://www.umanitoba.ca/faculties/architecture/cast/CASTonline.html; [Accessed: 11 November 2003]. A copy of this document is available from the author.

[6] West, Mark. June 2004. "Fabric-Formed Concrete Columns for Casa Dent in Culebra Puerto Rico." *Concrete International* Vol. 26(6), pp. 42+.

[7] West, Mark. April 2004. "Prestressed Fabric Formwork for Precast Concrete Panels." *Concrete International* Vol. 26(4), pp. 60+.

[8] Amoco Fabrics and Fibers Company. 1996. "Geosynthetile Properties: "Typical" & "Minimum Average Roll" Values." Technical Note No. 11. Atlanta, Georgia: Amoco Fabrics and Fibers Company. [Internet, WWW]. *Address:* http://www.geotextile.com/tech/tech.htm; [Accessed: 27 June 2004]. A copy of this document is available from the author.

[9] Amoco Fabrics and Fibers Company. 1996. "Tensile Tests for Geotextiles." Technical Note No. 19. Atlanta, Georgia: Amoco Fabrics and Fibers Company. [Internet, WWW]. *Address:* http://www.geotextile.com/tech/tech.htm; [Accessed: 5 May 2004]. A copy of this document is available from the author.

[10] Soderman, K.L. and J.P. Giroud. 1995. "Relationships Between Uniaxial and Biaxial Stresses and Strains in Geosynthetics." *Geosynthetics International* Vol. 2(2), pp. 495-504.

[11] Kaliakin, V.N., M. Dechasakulsom and D. Leshchinsky. 2000. "Investigation of the Isochrone Concept for Predicting Relaxation of Geogrids." *Geosynthetics International* Vol. 7(2), pp. 79-99.

[12] ASTM International. ASTM Committee D35 on Geosynthetics. 2001. *Test Method for Tensile Properties of Geotextiles by the Wide Width Strip Method*, Designation: D 4595-86 (Reapproved 2001). In Annual Book of ASTM Standards 2001. Vol. 4.13: Geosynthetics. West Conshohocken, Pennsylvania: ASTM International, pp. 1-10. [Internet, WWW, PDF]. *Available*: Available in .PDF format; *Address*: http://www.astm.org/cgi-bin/SoftCart.exe/index.shtml?E+mystore; [Accessed: 29 June 2004].

[13] Geosynthetic Research Institute. July 2000. "GRI Test Method GS10." Standard Test Method for Accelerated Tensile Creep and Creep-Rupture of Geosynthetic Materials Based on Time-Temperature Superposition Using the Stepped Isothermal Method. Drexel University, Folsom, Pennsylvania. pp. GS10 – 1-15. [Internet, WWW]. *Address*: http://www.drexel.edu/gri/; [Accessed: 28 June 2004]. A copy of this document is available from the author.

[14] ADINA R & D, Inc. June 2003. *ADINA* (Version 8.1.0). [Computer program]. *Available*: ADINA R & D, Inc., 71 Elton Avenue, Watertown, Massachusetts 02472.

[15] ADINA R & D, Inc. June 2003. *ADINA – Theory and Modeling Guide.* Report ARD 03-7. Watertown, Massachusetts: ADINA R & D, Inc.

[16] ADINA R & D, Inc. June 2003. *ADINA – User Interface Command Reference Manual.* Report ARD 03-2. Watertown, Massachusetts: ADINA R & D, Inc.

[17] Bathe, Klaus-Jürgen. 1996. *Finite Element Procedures.* Upper Saddle River, New Jersey: Prentice-Hall, Inc.

[18] Baker, Thomas L. 2002. *Amoco 2006 Stress-Strain*. Atlanta, Georgia: Amoco Fabrics and Fibers Company. [Internet, e-mail to the author]. *Available*: A copy of this e-mail message is available from the author at rpschmitz@wi.rr.com.

[19] ACI Committee 318. 2002. *Building Code Requirements for Structural Concrete (ACI 318-02) and Commentary (ACI 318R-02)*. Farmington Hills, Michigan: American Concrete Institute.

APPENDIX A

GENERAL DISCUSSION OF CREEP IN GEOTEXTILE FABRICS.

Creep in Geotextile Fabrics

The effects of creep in the geotextile fabric were not included in the modeling of the fabric panel but a general discussion will be given as a point of reference for future considerations. Long-term effects of creep are typically of concern in geotechnical projects.[1] For this application the fabric is expected to be under load for a relatively short period of time, perhaps as little as 24 hours, especially when high-early cement is used and creep in the fabric is not anticipated to play a major role.

There are three temperature dependent phases in geotextiles. These phases are the elastic phase, visco-elastic phase and liquid phase. The temperature defining the elastic/visco-elastic phase is the Glass Transition Temperature, which for polypropylene tapes is 0° F. The temperature defining the visco-elastic/liquid phase is the Melting Point Temperature, which for polypropylene tapes is 347° F. Creep will contribute to fabric deformation when the material is in the visco-elastic phase.[2]

Isochronous creep curves and creep coefficient curves are used to estimate total and creep extensions at different stress levels over time.[2] The creep coefficient is a measure of the rate of creep and is dependent on the stress level in the material. Creep test results for the Amoco 2006 geotextile fabric were obtained from Amoco Fabrics and Fibers Company. Figure A1 shows the Creep Test result curves for tests in the FILL direction (cross machine direction). Figure A1 also shows the construction of the creep coefficient, b_{25}, for the material being stressed at a constant rate of 25% of its ultimate load in the FILL direction. Figure A2 shows the Creep Test result curves for tests in the WARP direction (machine direction). The construction of the creep coefficient, b_{15}, for the material being stressed at a constant rate of 15% of its ultimate load in the WARP direction is also shown in Figure A2. ASTM D5262 is the standard test method used when evaluating creep in geosynthetics.[3] Total strain in the fabric is defined by (A-1).

$$\varepsilon_t = \varepsilon_0 + b \log t \qquad \text{(A-1)}$$

where

ε_0 is the initial strain,
b is the creep coefficient,
t is time.

Should creep need to be taken into account in future studies, adjustments to the tensile modulus of elasticity during the iterative process would be required.

---

[1] Amoco Fabrics and Fibers Company, October 1998, "Long-Term Design Strength Properties of Reinforcement Geotextile," Technical Bulletin, (Atlanta, GA: Amoco Fabrics and Fibers Company), p. 1. [Internet, WWW]. *Address:* http://www.geotextile.com/tech/tech.htm; [Accessed: 5 May 2004]. A copy of this document is available from the author.

[2] Terram Ltd., May 2000, "Designing for Soil Reinforcement (Steep Slopes)," Handbook, (United Kingdom: Terram Ltd.), pp. 19-22. [Internet, WWW]. *Address:* http://www.terram.co.uk; [Accessed: 2 July 2004]. A copy of this document is available from the author.

[3] ASTM International, ASTM Committee D35 on Geosynthetics, 2002, *Test Method for Evaluating the Unconfined Tension Creep Behavior of Geosynthetics,* Designation: D 5262-02a, In Annual Book of ASTM Standards 2002, Section 4: Construction, Volume 4.13: Geosynthetics, (West Conshohocken, PA: ASTM International), pp. 1-8. [Internet, WWW, PDF]. *Available*: Available in .PDF format; *Address:* http://www.astm.org/cgi-bin/SoftCart.exe/index.shtml?E+mystore; [Accessed: 7 July 2004].

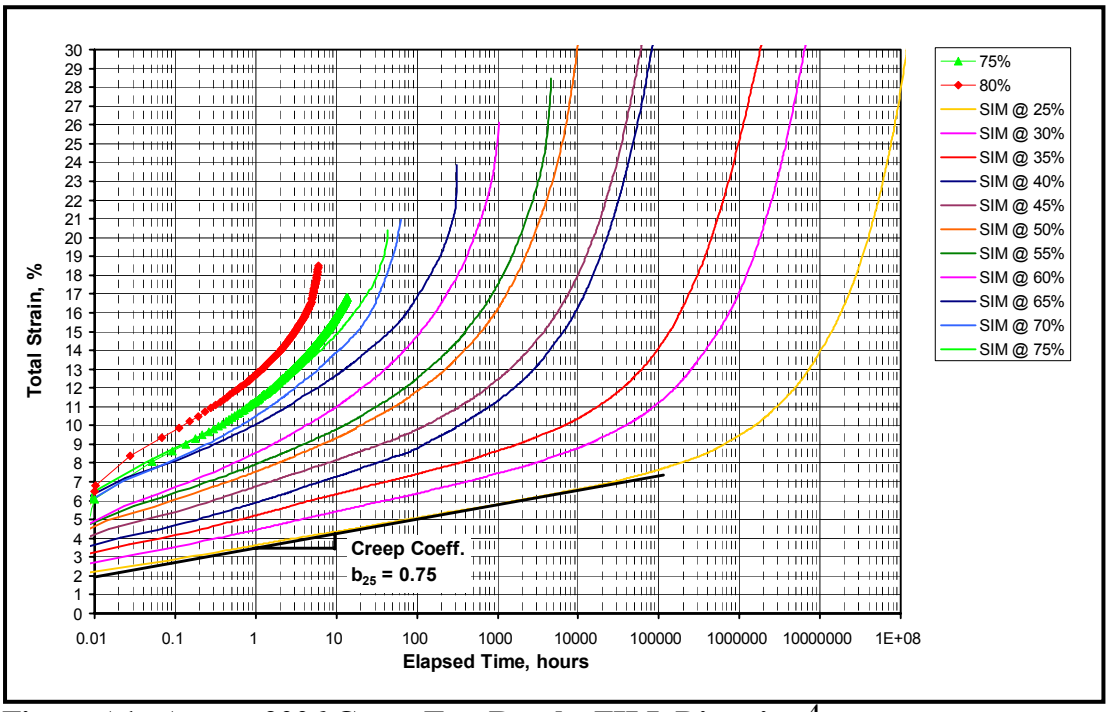

Figure A1. Amoco 2006 Creep Test Results FILL Direction.[4]

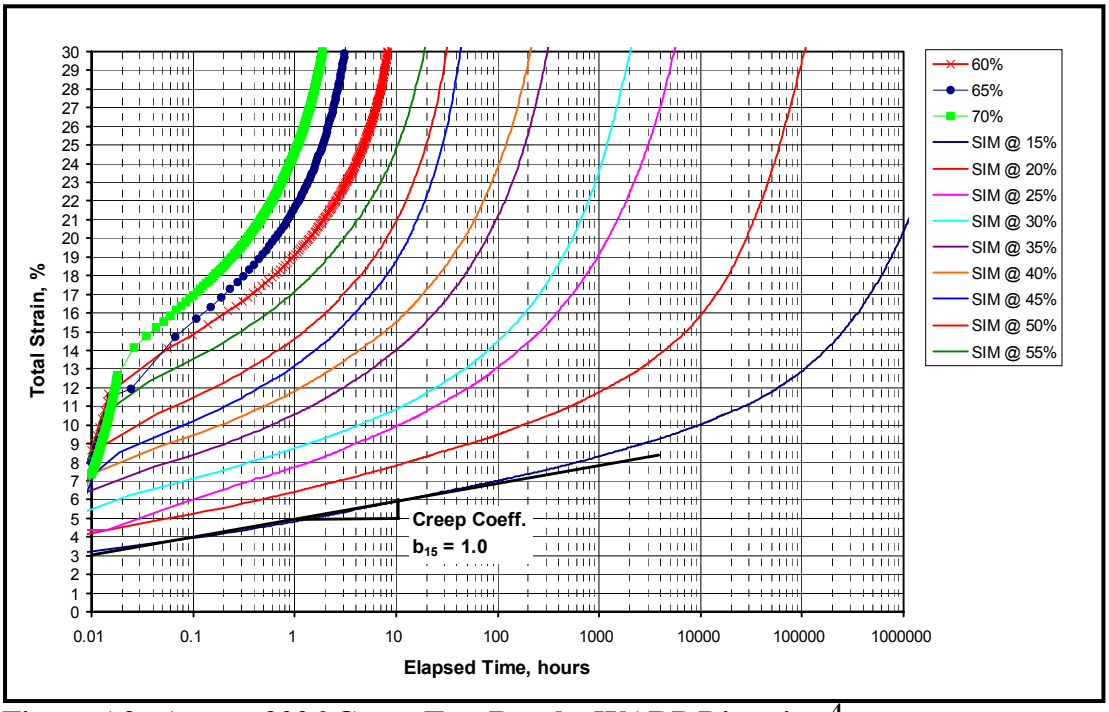

Figure A2. Amoco 2006 Creep Test Results WARP Direction.[4]

[4] Baker, Thomas L., 2000, *Amoco 2006 Creep Results*, (Atlanta, GA: Amoco Fabrics and Fibers Company). [Internet, e-mail to the author]. *Available*: A copy of this e-mail message is available from the author at rpschmitz@wi.rr.com.

APPENDIX B

PANEL 3 SERIES MODELS AND LOAD PATHS FOR VARIOUS BOUNDARY CONDITIONS.

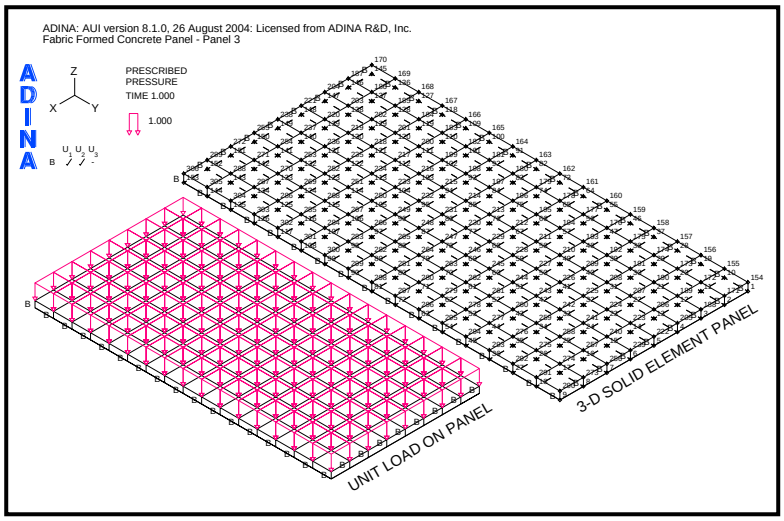

Figure B1. Panel 3 – Model.

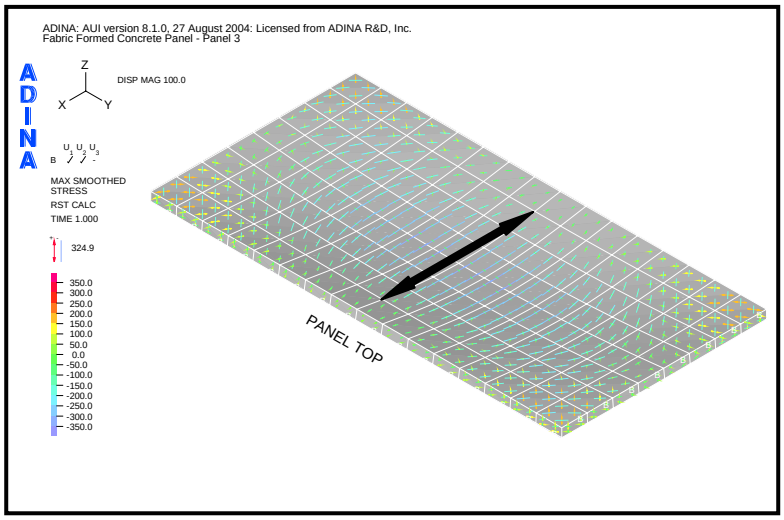

Figure B2. Panel 3 – Panel Top Load Paths.

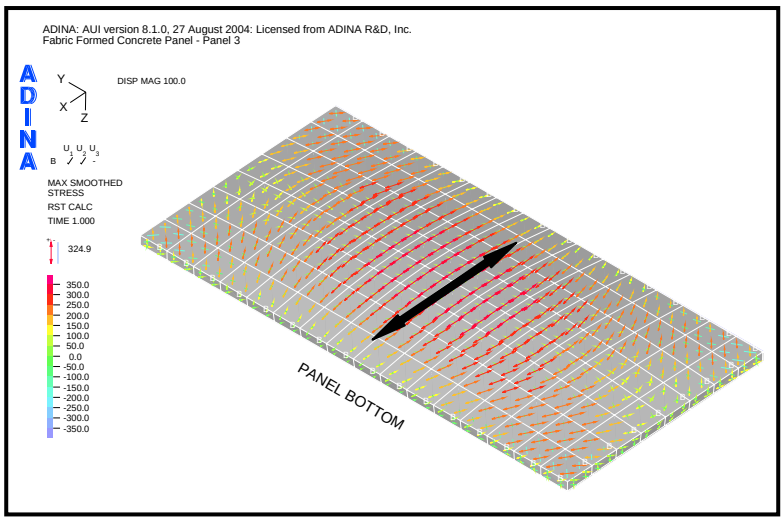

Figure B3. Panel 3 – Panel Bottom Load Paths.

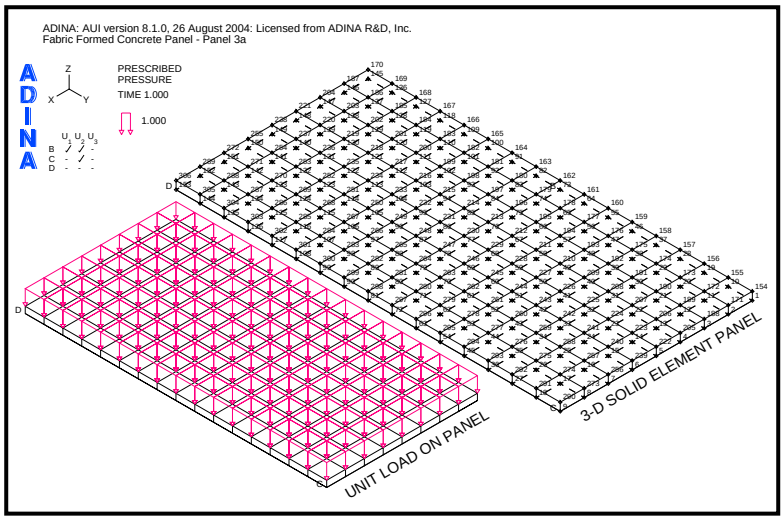

Figure B4. Panel 3a – Model.

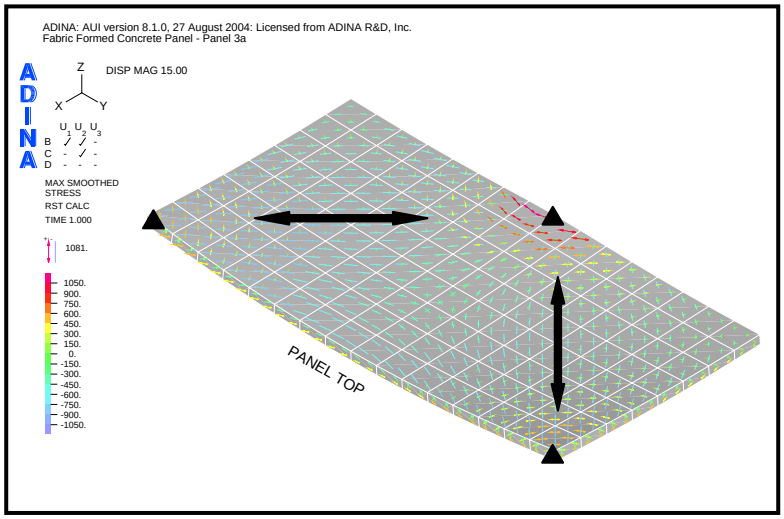

Figure B5. Panel 3a – Panel Top Load Paths.

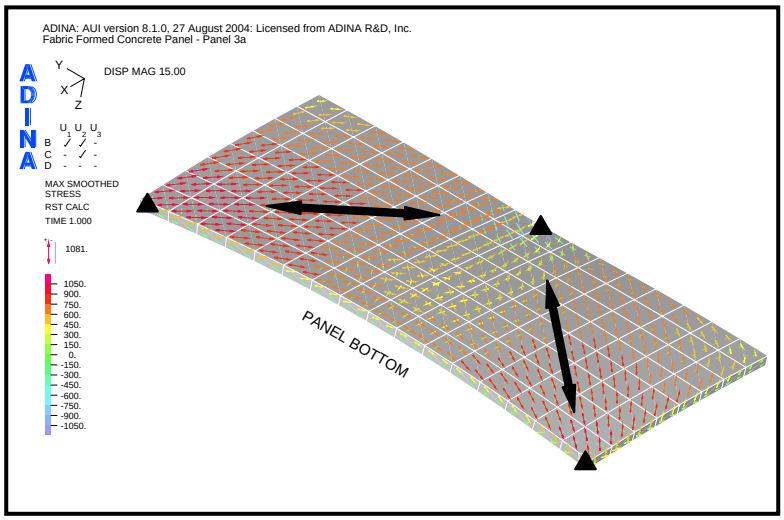

Figure B6. Panel 3a – Panel Bottom Load Paths.

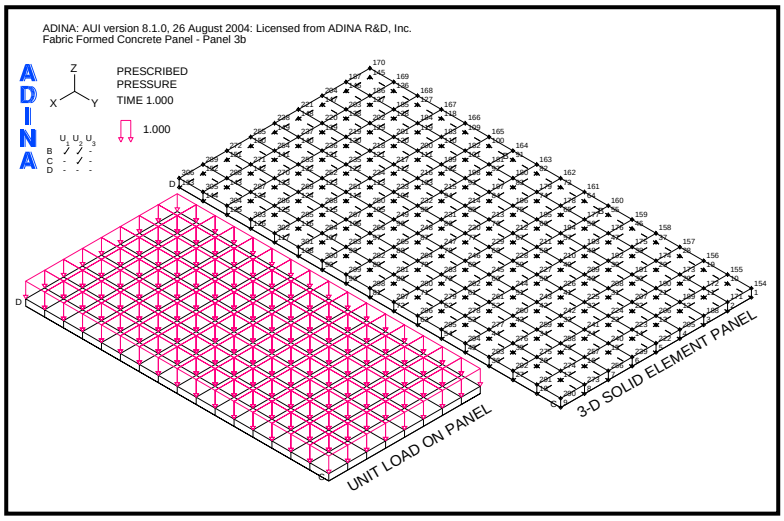

Figure B7. Panel 3b – Model.

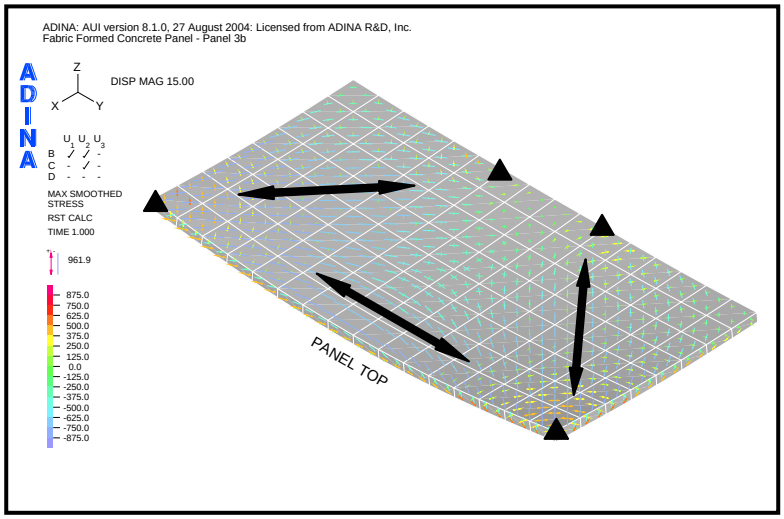

Figure B8. Panel 3b – Panel Top Load Paths.

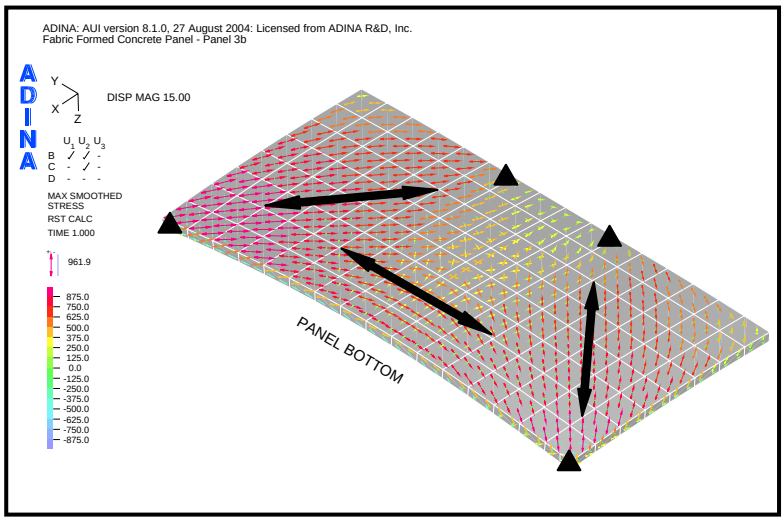

Figure B9. Panel 3b – Panel Bottom Load Paths.

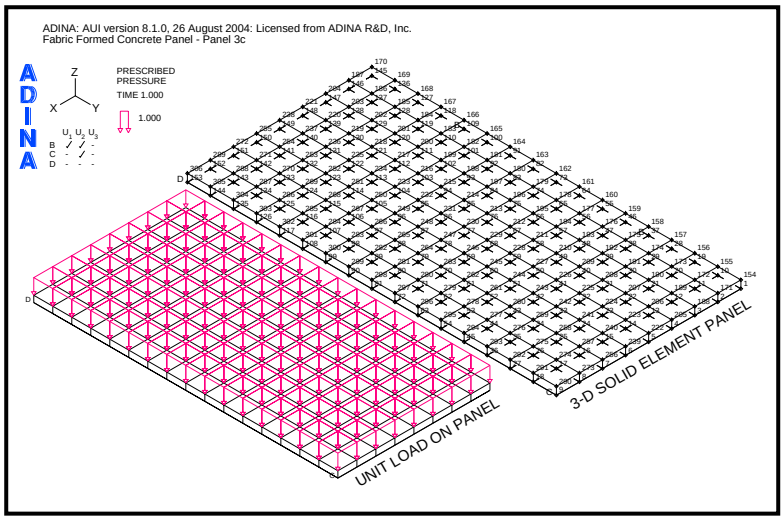

Figure B10. Panel 3c – Model.

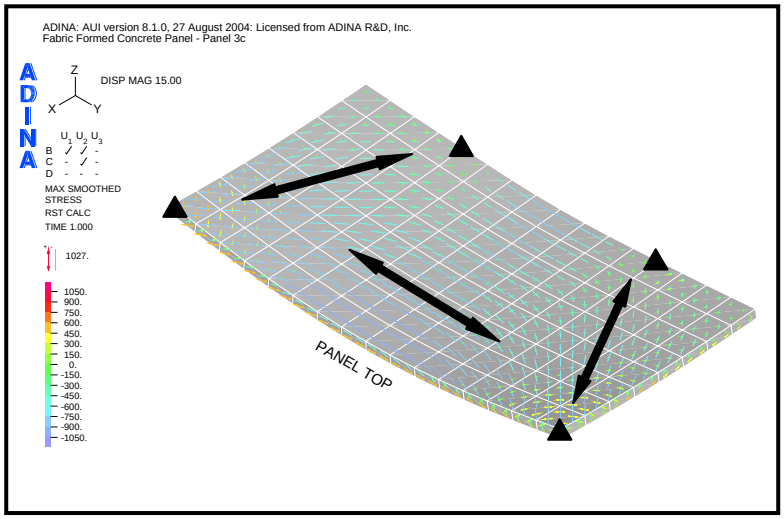

Figure B11. Panel 3c – Panel Top Load Paths.

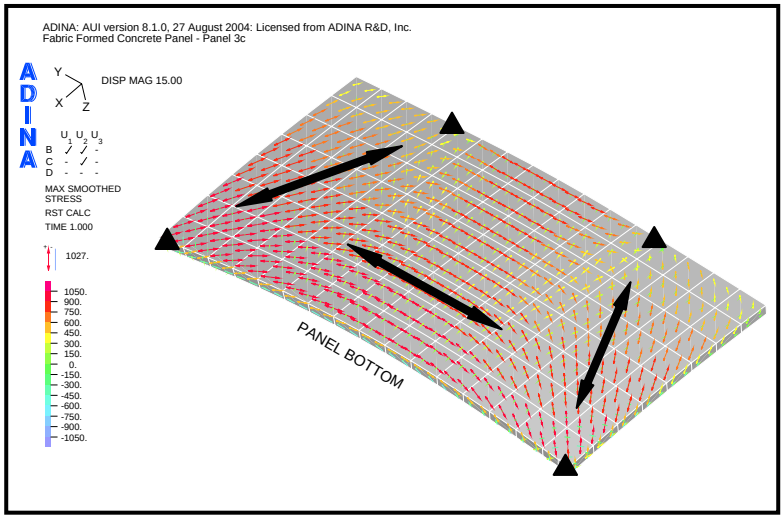

Figure B12. Panel 3c – Panel Bottom Load Paths.

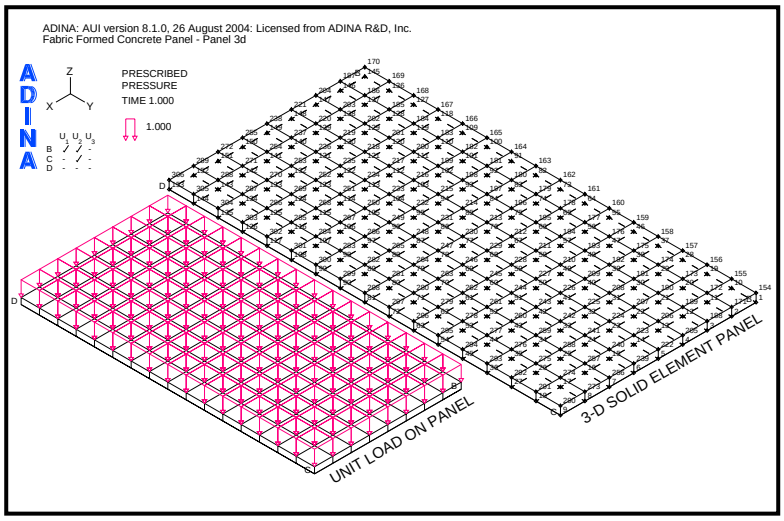

Figure B13. Panel 3d – Model.

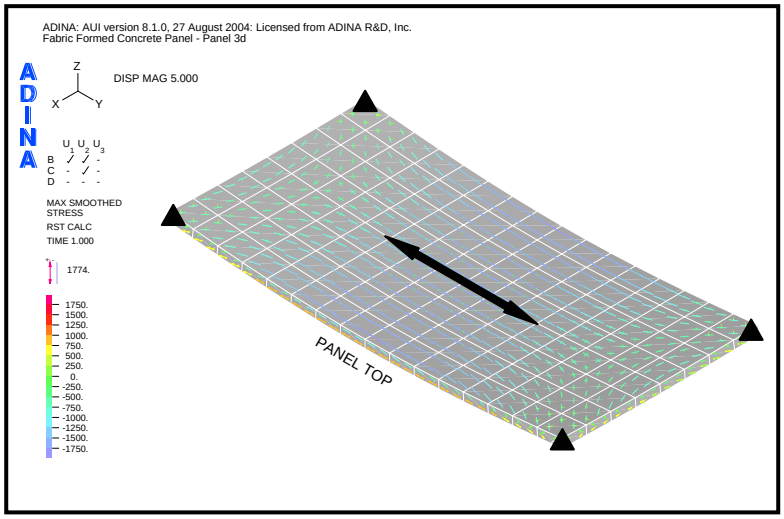

Figure B14. Panel 3d – Panel Top Load Paths.

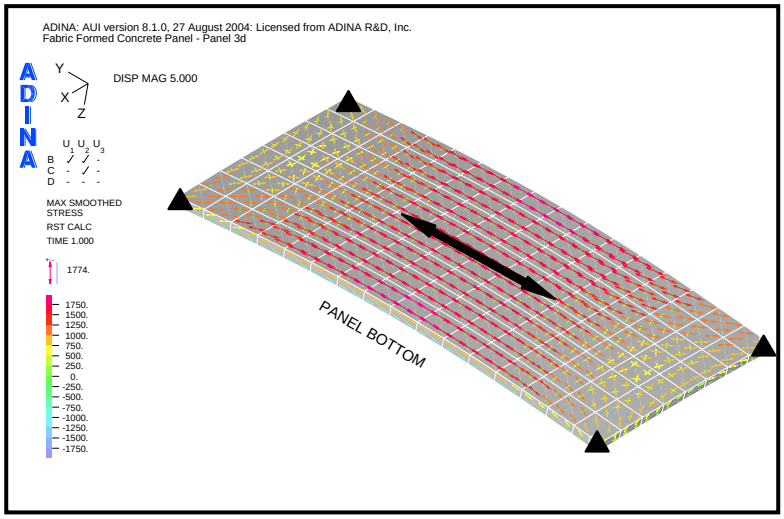

Figure B15. Panel 3d – Panel Bottom Load Paths.

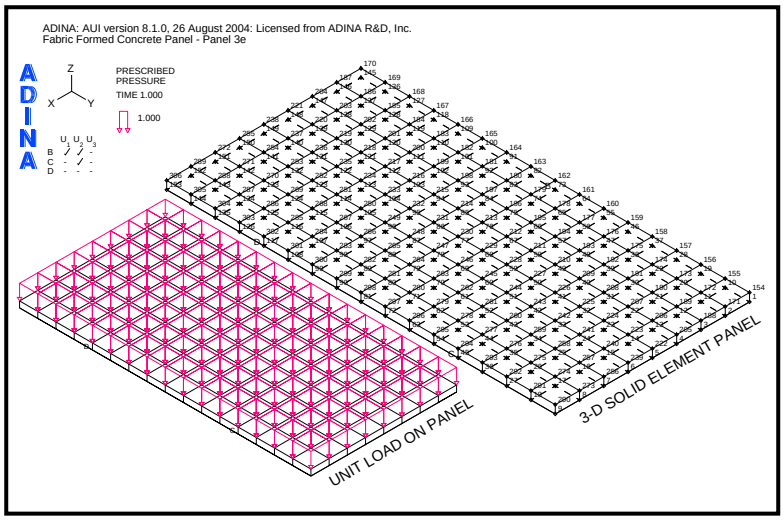

Figure B16. Panel 3e – Model.

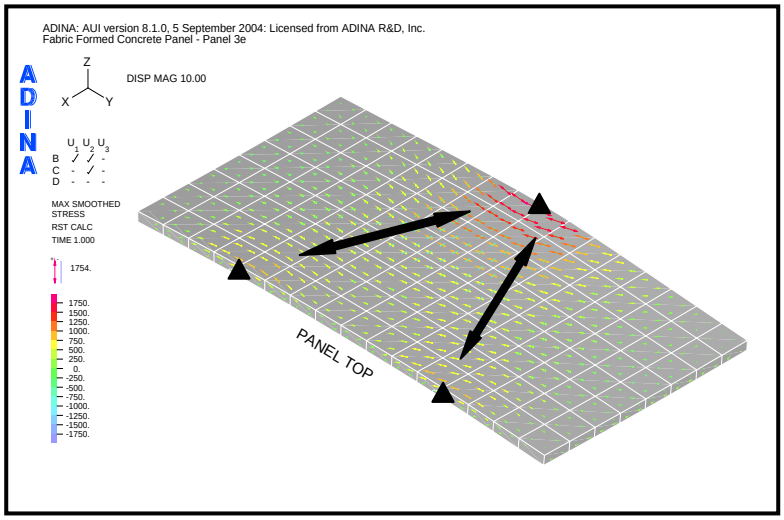

Figure B17. Panel 3e – Panel Top Load Paths.

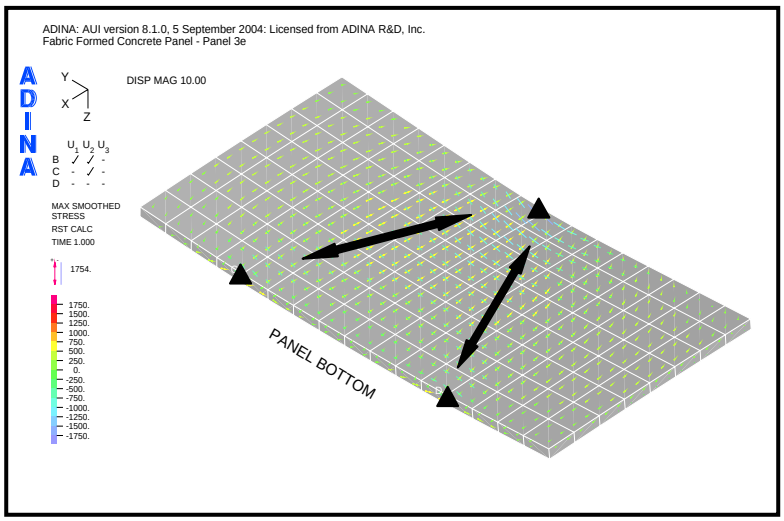

Figure B18. Panel 3e – Panel Bottom Load Paths.

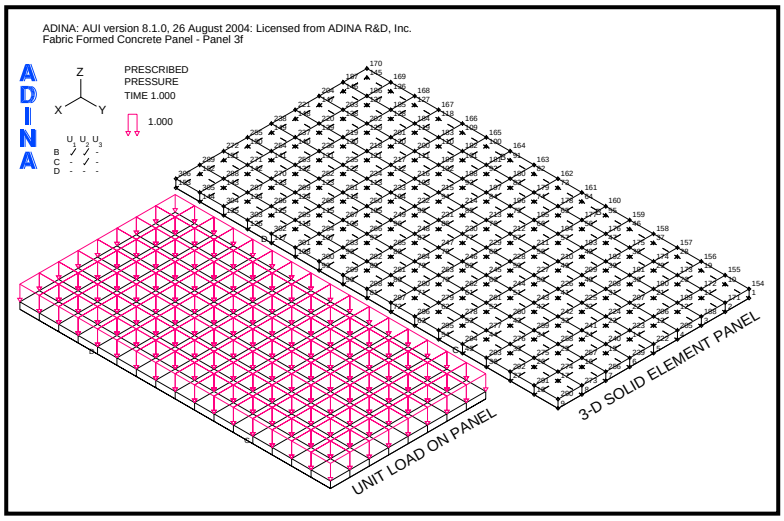

Figure B19. Panel 3f – Model.

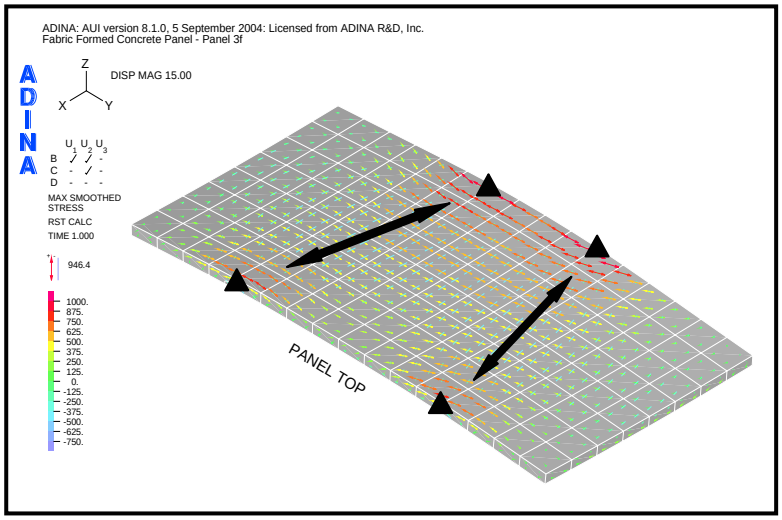

Figure B20. Panel 3f – Panel Top Load Paths.

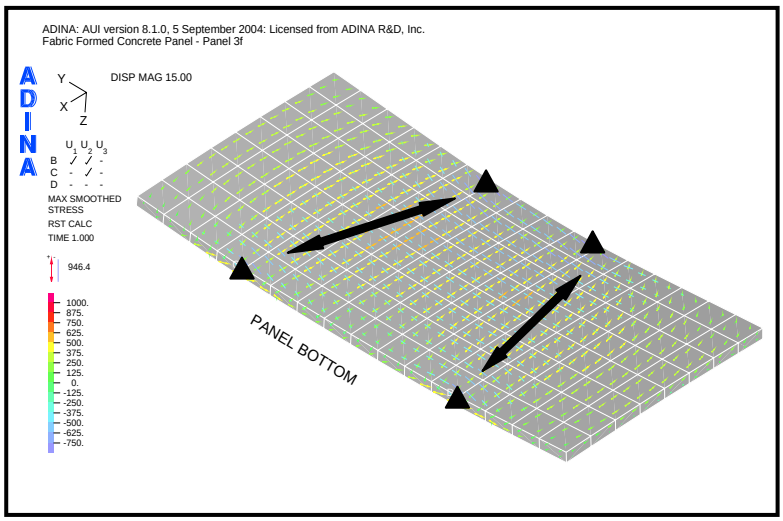

Figure B21. Panel 3f – Panel Bottom Load Paths.

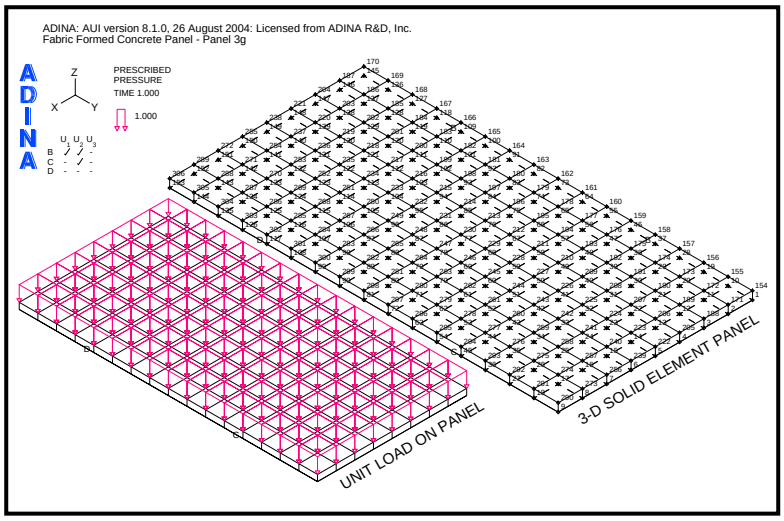

Figure B22. Panel 3g – Model.

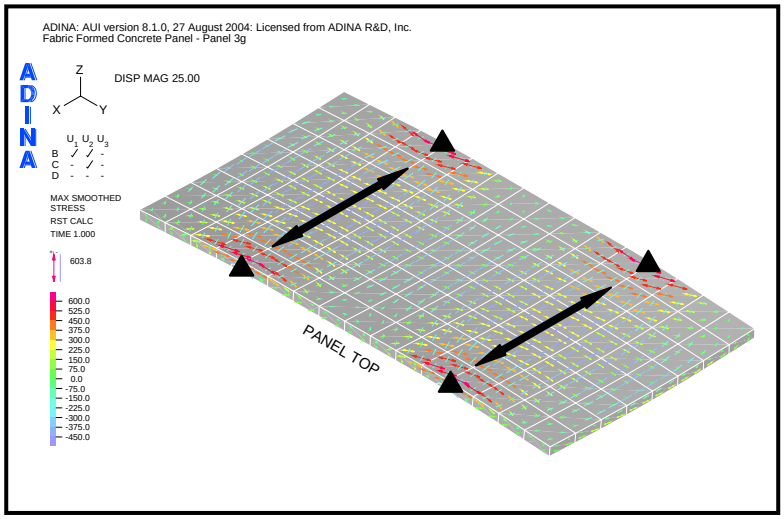

Figure B23. Panel 3g – Panel Top Load Paths.

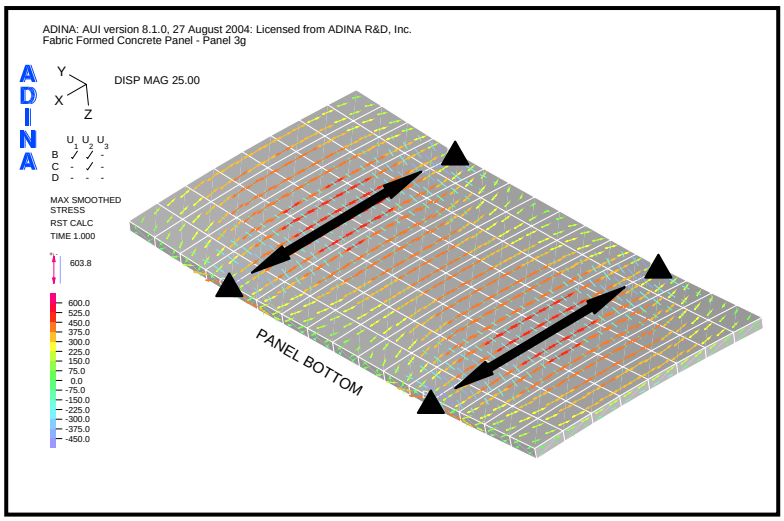

Figure B24. Panel 3g – Panel Bottom Load Paths.

APPENDIX C

CRACK PATTERNS FOR OVERLOAD CONDITIONS, PANELS 4, 5 AND 6.
CRACK PATTERNS FOR REINFORCED PANEL 5.

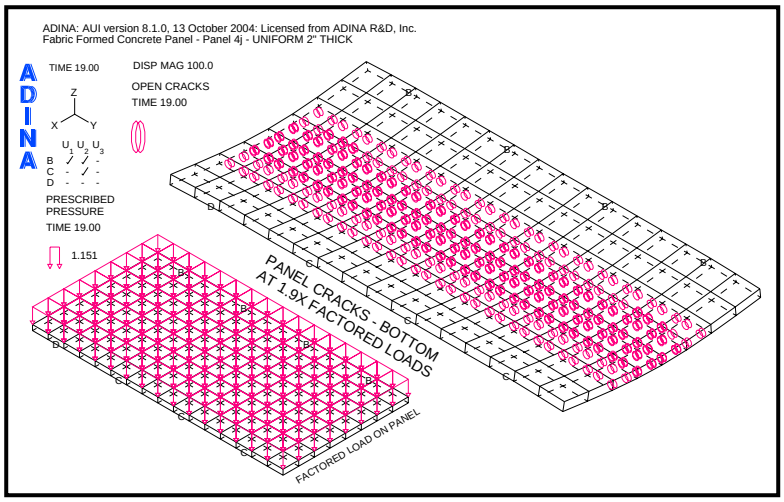

Figure C1. Panel 4 – Overload Cracks, Panel Bottom.

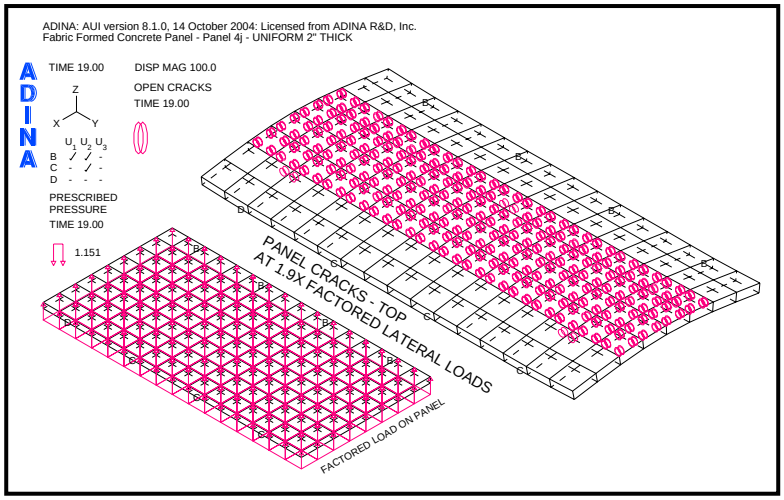

Figure C2. Panel 4 – Overload Cracks, Panel Top.

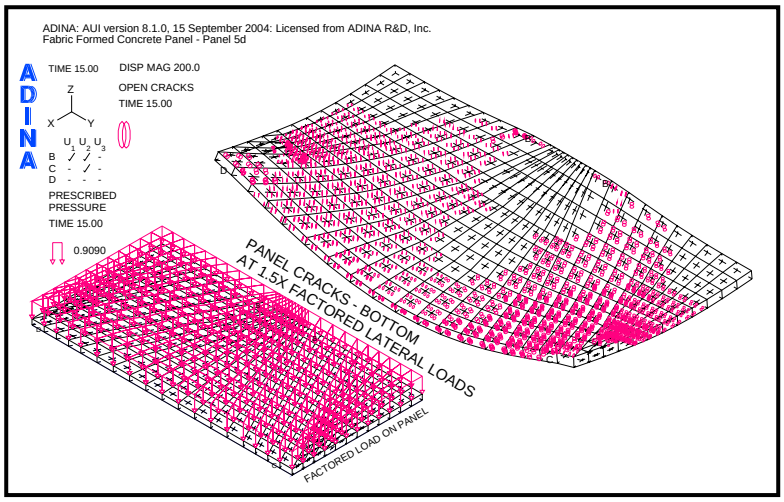

Figure C3. Panel 5 – Overload Cracks, Panel Bottom.

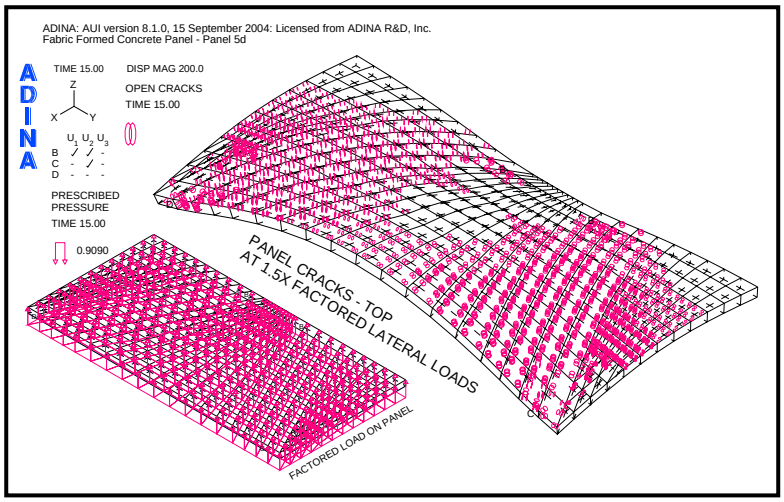

Figure C4. Panel 5 – Overload Cracks, Panel Top.

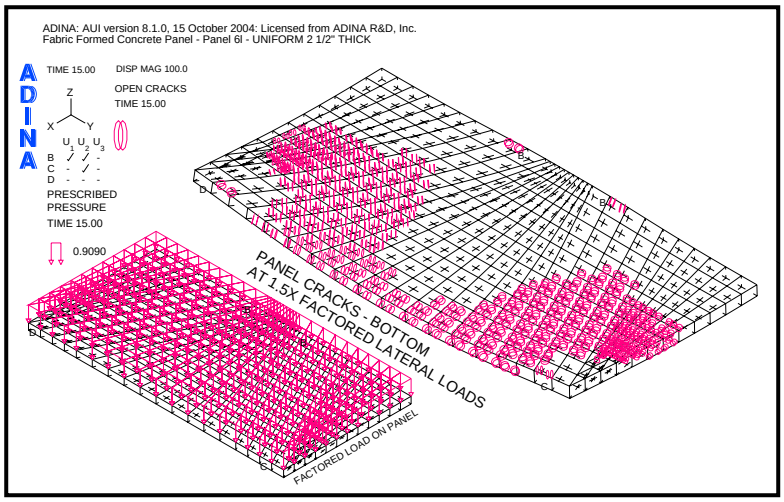

Figure C5. Panel 6 – Overload Cracks, Panel Bottom.

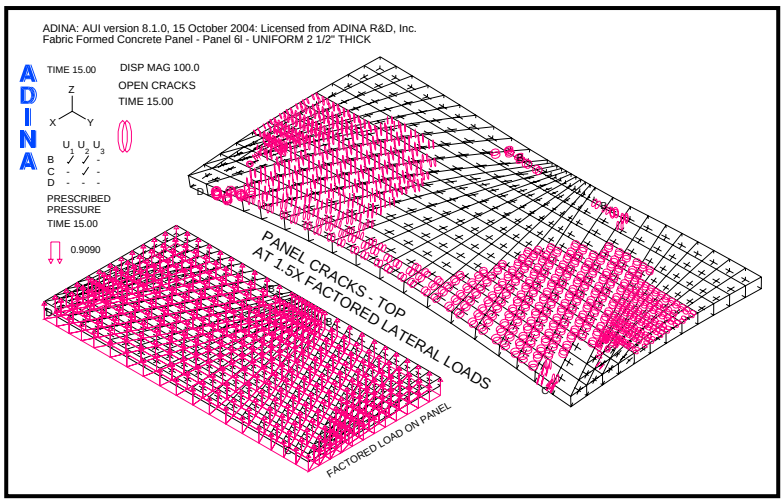

Figure C6. Panel 6 – Overload Cracks, Panel Top.

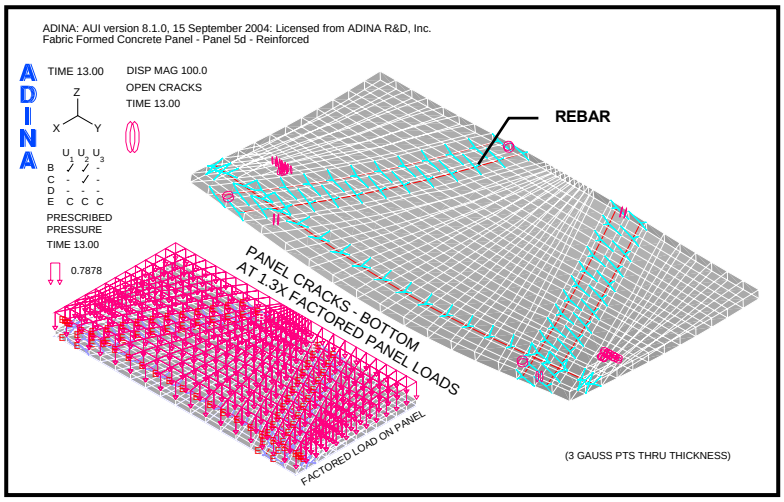

Figure C7. Reinforced Panel 5 – First Cracks, Panel Bottom.

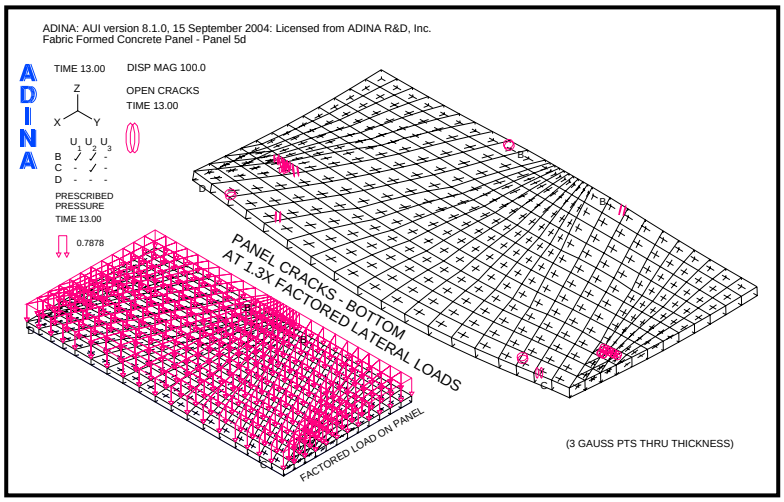

Figure C8. Plain Panel 5 – First Cracks, Panel Bottom.

The observation may be made that the crack patterns for both the reinforced and unreinforced concrete panels in Figures C7 and C8 are the same using a Gauss point integration order of three.

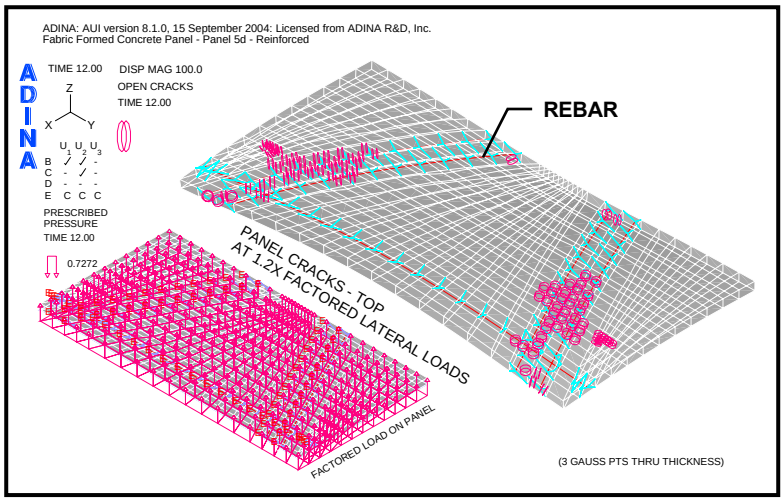

Figure C9. Reinforced Panel 5 – First Cracks, Panel Top.

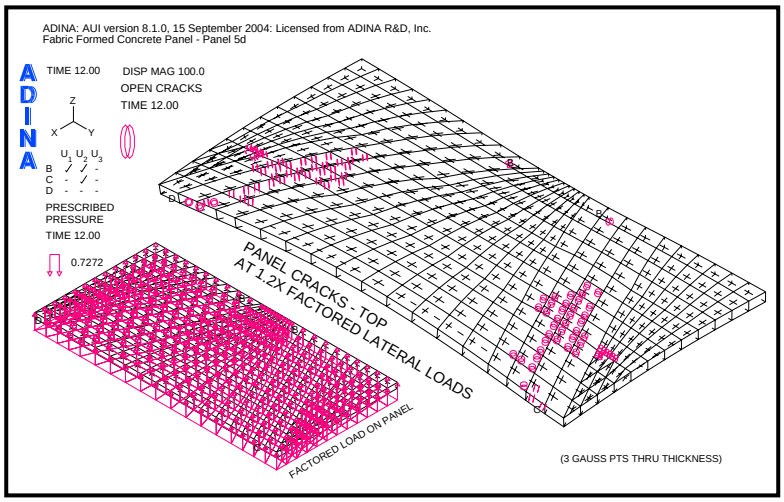

Figure C10. Plain Panel 5 – First Cracks, Panel Top.

The observation may be made that the crack patterns for both the reinforced and unreinforced concrete panels in Figures C9 and C10 are the same using a Gauss point integration order of three.

APPENDIX D

PANEL 5 – ¼–SCALE MODEL PHOTOS.

Figure D1. Panel 5 – Fabric Support Frame.

Figure D2. Panel 5 – Fabric Stretched onto Frame.

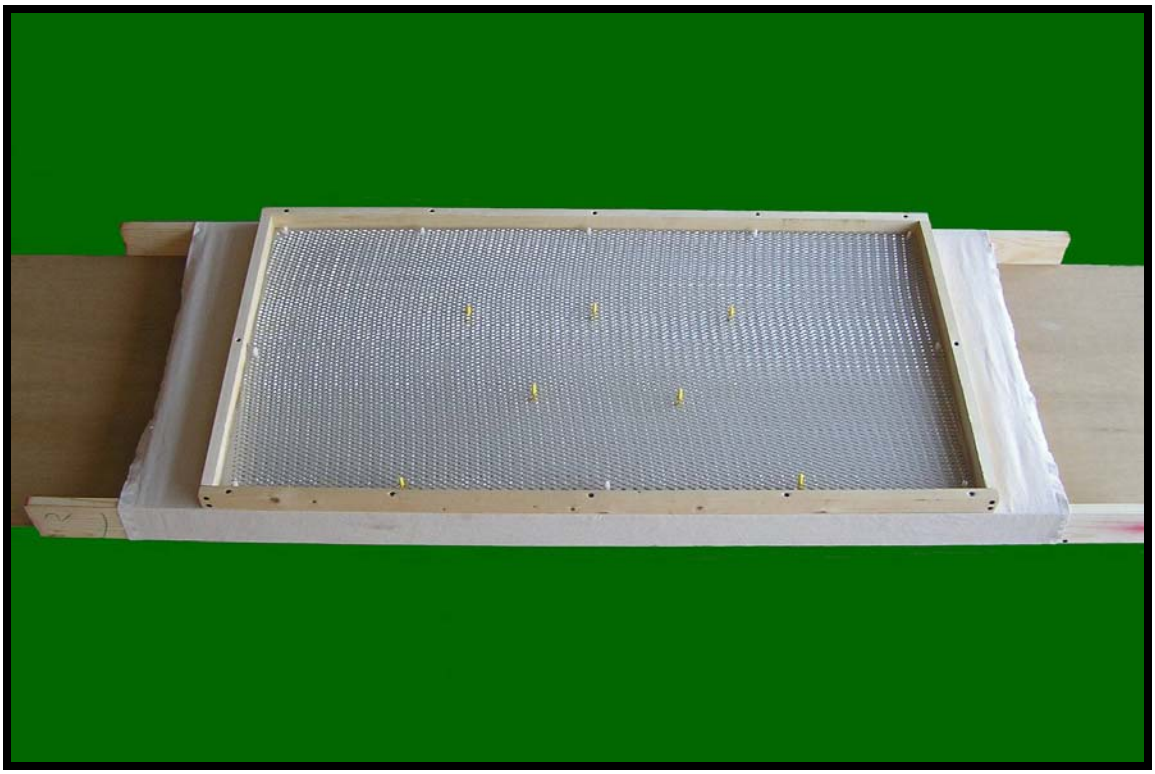

Figure D3. Panel 5 – Mesh over Fabric.

Figure D4. Panel 5 – Front View of Cast Panel.

Figure D5. Panel 5 – End View of Cast Panel.

STRUCTURAL ENGINEERING

FINAL DESIGN PROJECT REPORT APPROVAL FORM

Master of Science – Structural Engineering

Milwaukee School of Engineering

This report, for the project titled "Fabric-Formed Concrete Panel Design," submitted by the student Robert P. Schmitz, has been approved by the following committee:

Faculty Advisor: Dr. Peter Huttelmaier Date: 11/8/04

Faculty Member: Dr. Richard DeVries Date: 11/8/04

Faculty Member: Dr. Mahmoud Maamouri Date: 11/8/04